RSC Advances

REVIEW

View Article Online
View Journal | View Issue

Cite this: *RSC Adv.*, 2022, **12**, 12011

A review on α-glucosidase inhibitory activity of first row transition metal complexes: a futuristic strategy for treatment of type 2 diabetes

Marzieh Sohrabi,[a] Mohammad Reza Binaeizadeh,[b] Aida Iraji,[cde] Bagher Larijani,[a] Mina Saeedi *[fg] and Mohammad Mahdavi*[a]

Type 2 diabetes mellitus (T2DM) is characterized by high blood glucose levels and has emerged as a controversial public health issue worldwide. The increasing number of patients with T2DM on one hand, and serious long-term complications of the disease such as obesity, neuropathy, and vascular disorders on the other hand, have induced a huge economic impact on society globally. In this regard, inhibition of α-glucosidase, the enzyme responsible for the hydrolysis of carbohydrates in the body has been the main therapeutic approach to the treatment of T2DM. As α-glucosidase inhibitors (α-GIs) have occupied a special position in the current research and prescription drugs are generally α-GIs, researchers have been encouraged to design and synthesize novel and efficient inhibitors. Previously, the presence of a sugar moiety seemed to be crucial for designing α-GIs since they can attach to the carbohydrate binding site of the enzyme mimicking the structure of disaccharides or oligosaccharides. However, inhibitors lacking glycosyl structures have also shown potent inhibitory activity and development of non-sugar based inhibitors is accelerating. In this respect, *in vitro* anti-α-glucosidase activity of metal complexes has attracted lots of attention and this paper has reviewed the inhibitory activity of first-row transition metal complexes toward α-glucosidase and discussed their probable mechanisms of action.

Received 5th January 2022
Accepted 12th April 2022

DOI: 10.1039/d2ra00067a

rsc.li/rsc-advances

Introduction

Diabetes mellitus (DM) is a chronic metabolic disease, known as one of the important causes of death in the world due to acute side effects.[1] The long-term high levels of blood glucose in patients with DM result in various disorders such as microvascular complications or destruction of very small blood vessels in the body causing serious kidney, eye, nerve and heart diseases.[2] There are two primary forms of diabetes including type 1 (T1DM) and type 2 (T2DM). T1DM is defined as an insulin-dependent form of the disease and T2DM is described as a non-insulin-dependent disorder.[3] The majority of the world's patients with T2DM and the prevalence of the disease have become an increasing public health issue. According to the prediction of the World Health Organization (WHO) in 2006, the number of patients with T2DM may increase to 366 million by 2030 which accounts for 9.9% of the world's adult population.[4] Several factors related to lifestyle such as (i) obesity and weight,[5,6] (ii) physical inactivity (independent of obesity),[7,8] (iii) cigarette smoking,[9] (iv) a low-fiber diet with a high glycemic index,[10] and (v) depression,[11] are involved in increasing the risk of T2DM.

Currently, lowering blood glucose levels has been known as the most effective anti-diabetic therapeutic tool.[12,13] At this juncture, α-glucosidase inhibitors (α-GIs) have occupied a special position in drug development research since α-glucosidase is a key enzyme converting complex carbohydrates (polysaccharides) into simple sugars (monosaccharides) (Fig. 1a and b).[14] α-Glucosidase located in the brush border of the small intestinal can selectively hydrolyze terminal (1 → 4)-linked α-glucosidase residues (starch or disaccharides), leading to the formation of glucose.[15,16] α-GIs can reduce the rate of glucose uptake by delaying the digestion of carbohydrates. Thus, reducing the effect of dietary carbohydrates on blood sugar has been revealed to be vital in avoiding the progression of impaired glucose tolerance factor (GTF) to T2DM. Generally, the basic modes of action of α-GIs can be competitive (Fig. 1c), non-competitive (allosteric) (Fig. 1d), and uncompetitive (Fig. 1e).

[a]*Endocrinology and Metabolism Research Center, Endocrinology and Metabolism Clinical Sciences Institute, Tehran University of Medical Sciences, Tehran, Iran. E-mail: momahdavi@tums.ac.ir*

[b]*School of Chemistry, College of Science, University of Tehran, Tehran, Iran*

[c]*Stem Cells Technology Research Center, Shiraz University of Medical Sciences, Shiraz, Iran*

[d]*Central Research Laboratory, Shiraz University of Medical Sciences, Shiraz, Iran*

[e]*Liosa Pharmed Parseh Company, Shiraz, Iran*

[f]*Medicinal Plants Research Center, Faculty of Pharmacy, Tehran University of Medical Sciences, Tehran, Iran . E-mail: m-saeedi@tums.ac.ir*

[g]*Persian Medicine and Pharmacy Research Center, Tehran University of Medical Sciences, Tehran, Iran*

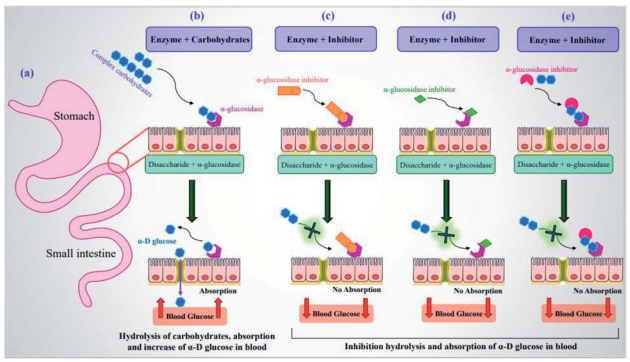

Fig. 1 (a) Schematic diagram of small intestine. (b) Hydrolysis of complex carbohydrates by α-glucosidase along the brush border of small intestine to release α-D-glucose. Basic modes of action of α-GIs: (c) competitive, (d) non-competitive, and (e) uncompetitive inhibition of α-glucosidase leading to decrease of postprandial blood glucose levels.

Conventional α-GIs are structurally similar to disaccharides or oligosaccharides, able to attach to the carbohydrate binding site of enzyme. Acarbose (glucobay), voglibose (volix, Basen), and miglitol (Glyset), are three prescription α-GIs available in the market and frequently used for the treatment of T2DM (Fig. 2). However, they suffer from various side effects specially gastrointestinal problems and following that, a wide range of studies have been conducted on the anti-α-glucosidase activity of natural[17–19] and synthetic heterocyclic compounds[20–27] since the efficacy of α-GIs in the treatment of T2DM has been completely proven. Biological activity of metal ions and their complexes[28,29] have made them an important topic in drug discovery research. Recently, they have been investigated for their anti-α-glucosidase activity and it is hoped that metallotherapy can open a new horizon in the field of anti-T2DM agents.

Biological activity of first-row transition metals

The 10 first-row transition metals (Sc, Ti, V, Cr, Mn, Fe, Co, Ni, Cu, and Zn) profit from both structural and functional roles to induce desired biological properties and diagnostic applications.[30,31] Among them, manganese, iron, cobalt, copper, and zinc are five essential elements to human health.[31] However, three first-row transition metals including chromium, vanadium, and nickel are generally used as nutritional additives in different diets and possess favorable.[30] The structural or catalytic function of these metal ions allows them to bind to the proteins, DNA, RNA or other biological structures to be able to exert a certain role.

Oxidation state of the metal center especially that of transition metal complexes plays a significant role in the induction of medicinal properties. The redox environment and the nature of the ligands as well as the group number of metal center lead to different oxidation states of the first-row transition metal complexes.[32]

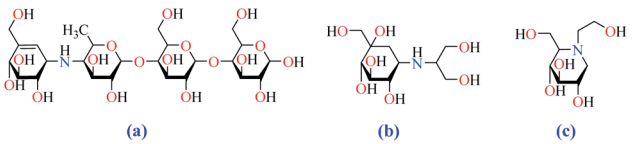

Fig. 2 Chemical structures of clinically used α-GIs, (a) acarbose, (b) voglibose, and (c) miglitol.

The idea of using metal ions to treat diabetes dates back to 1899 and the anti-diabetic properties of the orally active metal complexes such as oxovanadium(IV) (vanadyl) were initially considered in 1990.[33,34]

In 1979, vanadium salts were reported to have *in vitro* insulin-mimetic effects[35] and their insulin-like activity was revealed in 1899.[36] However, vanadium's pharmacological potential was systematically investigated by Heyliger *et al.*[37] Bis(2-ethyl-3-hydroxy-4-pyronato)oxovanadium(IV) (BMOV) which was first synthesized in the late 1990s,[38,39] showed desired activity on STZ diabetic rats, possessing higher potency and efficacy than a common inorganic vanadium salt.[40] Bis(ethylmaltolato)oxidovanadium(IV) (BEOV) was also found to be anti-diabetic agent derived from vanadium.[41] Also, different vanadium, copper and zinc metal complexes[42] were found to be effective for the treatment of diabetes under *in vivo* conditions.[33]

Mechanistic role of the metal center in the inhibitory activity of the corresponding complexes was completely reviewed by Dyson *et al.*[43] Subsequently, metal complexes are divided into three main classes: (I) metal complexes having biologically active ligands (non-innocent ligands): in this group, metal centers have a structural role and unlike ligands that are biologically active components, they do not play a role in the enzyme inhibition. However, the metal center can indirectly affect the binding of ligand to the enzyme by undergoing a redox process. (II) Metal complexes having biologically active metal center (innocent ligands): in this class of compounds, ligands are usually biologically inactive and their main role is only masking and stabling the metal ion. (III) Metal complexes having biologically active metal and ligands: these metal complexes are predicted to have synergistic effects in inhibiting enzymes due to the biological effects of both metal ion and ligands. However, the mechanism of action of metal complexes in the inhibition of α-glucosidase has not been definitely reported in the literature.

In this review, α-glucosidase inhibitory activity of the first-row transition metal complexes (Zn, Cu, Ni, Co, Fe, Mn, Cr, V) with different oxidation states (II, III, and IV) was in the center of attention as they have shown potent activity and can be considered as novel and efficient surrogates of organic small molecules in the treatment of T2DM. For this purpose, discussed complexes were categorized into three classes based on the oxidation state of the central metal including divalent, trivalent, and tetravalent metal complexes. Moreover, to get better insight into the mechanism of action of metal complexes, docking study was performed for some selected complexes which confirmed the construction of desired interactions with the enzyme.

Divalent metal complexes as α-glucosidase inhibitors

Although some metal(II) ions and their complexes have demonstrated anti-diabetes properties,[44–46] their mechanism of

action is not completely clear. For example, manganese has played a significant role in the glucose metabolism[45] and zinc(II) complexes have shown an insulin-like effect on rat adipocytes.[47] In 1980, Coulston and Dandona reported that zinc could stimulate lipogenesis in rat adipocytes similar to the function of insulin.[48] Recently, various studies have reported anti-α-glucosidase activity of divalent first row transition metals (Zn(II), Cu(II), Ni(II), Co(II), Fe(II), and Mn(II)) complexes as listed in Tables 1–4 and Fig. 3. The complexes were categorized based on the functional group of ligands such as hydrazides, picolinic acids (PicAs), Schiff bases, and diamines coordinated to the metal(II) ions. These organic ligands generally have not demonstrated α-glucosidase inhibitory activity while the corresponding complexes have shown potent inhibitory activity.

Hydrazide metal(II) complexes

Bioactive compounds containing hydrazide moiety have shown extensive biological properties such as anti-cancer, anti-viral, analgesic and anti-inflammatory, anti-platelet, vasodilator, antioxidant, and hypoglycemic activities.[49] They are popular in coordination chemistry due to their ease of synthesis and electronic properties, inducing versatile enzymes inhibitory activity[50] through proper binding with the active sites. Hydrazide derivatives have been documented as a potent moiety for the inhibition of α-glucosidase.[51,52]

In this section, various metal(II) complexes containing different hydrazide moieties as a ligand were discussed[53–55] (Table 1). It should be noted that the results reported by Naik *et al.*[55] (Table 1, entry 4) had ambiguous values of IC_{50} or percent inhibition which led us to exclude those data and prevented authors from having a discussion based on the SAR. However, in this study, all complexes showed more potent activity than the free ligand.

Zinc(II) complexes. Khan *et al.* reported the synthesis of a novel series of 2-acetylbenzofuran hydrazides (**L1–L6**, Table 1, entry 1) to prepare the Zn(II) complexes (**1–6**, Table 1, entry 2a) to investigate anti-α-glucosidase activity[53] comparing with acarbose as the reference drug (IC_{50} = 378.25 μM). It was perceived that the synthesized complexes were generally more potent than the corresponding free ligands except complex **5**. It should be noted that **L1**, **L2**, **L4**, and **L5** were completely inactive, however, **L3** showed good activity with IC_{50} = 47.51 μM and **L6** was weak inhibitor of α-glucosidase (IC_{50} = 396.35 μM). Most Zn(II) complexes were found to be more potent than acarbose and among them, complexes **2** and **3** were the most active compounds with IC_{50} values of 56.27 and 27.71 μM, respectively. It seems that the presence of strong electron-withdrawing group (pyridine moiety and NO_2, **L2** and **L3**) played a significant role in the induction of anti-α-glucosidase activity by complexes. Change of the position of nitro group from 4- to 2- led to the reduction of activity of **4**. The presence of halogens and electron-releasing group (NH_2) led to lower activity. In the case of free ligands, **L1** and **L2** containing pyridine moiety at different positions were found to be inactive, while **L3** showed the most potent activity.

α-Glucosidase inhibitory activity of Zn(II) complexes **7** and **8** (Table 1, entries 3a and 3c) were also evaluated (IC_{50} = 180 and 190 μM, respectively) by Philip *et al.*,[54] and compared with acarbose (IC_{50} = 99 μM). Complexes were prepared *via* the coordination of chromone hydrazones ligands (**L8** and **L9**, Table 1, entry 1) and Zn(II). Inhibitory activity of **L8** and **L9** was approximately similar to each other (IC_{50} = 240 and 230 μM, respectively), however, weaker than the corresponding complexes. It should be mentioned that **L9** possessing phenolic OH group showed no higher activity than **L8** lacking hydroxyl group, a potent group for the construction of H-bonding interaction. However, coordination of the Zn(II) had no significant effect on the inhibitory effect. It seems that the formation of complex did not afford either structural or functional role.

Copper(II) complexes. Cu(II) complexes (**9–15**, Table 1, entry 2b) of 2-acetylbenzofuran hydrazides (**L1–L7**) were reported and evaluated for their α-glucosidase inhibitory activity compared with acarbose (IC_{50} = 378.25 μM).[53] All complexes were found to be more potent than free ligands. All of them except **9** and **15**, were potent inhibitors and among them, complexes **11**, **13**, and **14** showed the strongest inhibitory effect with IC_{50} values of 1.15, 0.15, and 0.21 μM respectively. In contrast to series of Zn(II) complexes, coordination of **L5** possessing strong electron-releasing group (NH_2) demonstrated the most potent activity, 7 times more potent than **11** having NO_2. Interestingly, **L5** possessing NH_2 group was inactive toward α-glucosidase. Among coordinated ligands to Cu(II), $[Cu(L6)_2]Cl_2$ **14** (IC_{50} = 0.21 μM) was found to be approximately as potent as **13** (IC_{50} = 0.15 μM). In the case of **L7** which showed no inhibitory activity, the related complex **15** was also inactive. Comparing inhibitory activity of **11** and **12** revealed that **11** (IC_{50} = 1.15 μM) was 16 times more potent than **12** (IC_{50} = 18.91 μM). In the series of Cu(II) complexes possessing 2-acetylbenzofuran hydrazide, the role of electronic effects of ligands is a key factor in the induction of inhibitory activity. The electronic effects of substituents on the aryl ring are directly affected by the position of substituents as the desired electron releasing or withdrawing is achieved *via* resonance or induction effects.

Using **L8** and **L9** containing a chromenone hydrazone moiety in the synthesis of complexes **16** and **17** (IC_{50}s = 140 and 170 μM, respectively, Table 1, entries 3b and 3d) as reported by Philip *et al.*,[54] led to the reduction of anti-α-glucosidase activity comparing with complex **13** (IC_{50} = 0.15 μM).

Similar to Zn(II) complexes (**7** and **8**), the inhibitory activity of their counterparts (**16** and **17**) was independent of phenolic OH group of the ligand. In addition, the narrow IC_{50} range of complexes **7**, **8**, **16**, and **17** suggested that the structural properties of complexes do not play a role in the inhibitory activity as **7** and **8** are disordered tetrahedral, **16** and **17** are disordered octahedral.

Nickel(II) complexes. Chromenone hydrazone ligands **L8** and **L9**, have been also used for the preparation of Ni(II) metal complexes **19** and **20** (Table 1, entries 3b and 3d),[54] to evaluate their anti-glucosidase activity. They showed moderate inhibitory activity and no significant difference was observed between the potency of **19** and **20** since the IC_{50} values were calculated as 200 and 230 μM, respectively, compared with acarbose (IC_{50} = 99 μM).

Table 1 α-Glucosidase inhibitory activity of divalent metal complexes bearing hydrazide ligands

Entry	Compounds	Structure number	IC_{50} (μM)	Ref.
1	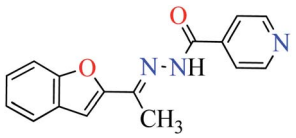	**L1**	NA	53[a]
	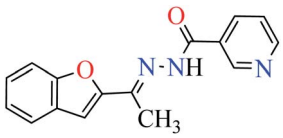	**L2**	NA	
	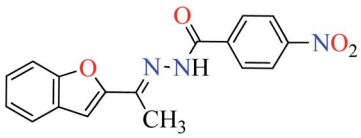	**L3**	47.51	
	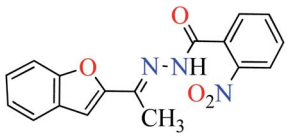	**L4**	NA	
	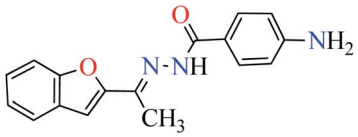	**L5**	NA	
	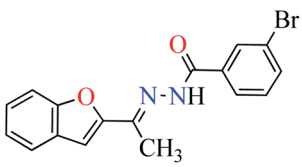	**L6**	396.35	
	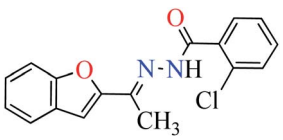	**L7**	NA	
	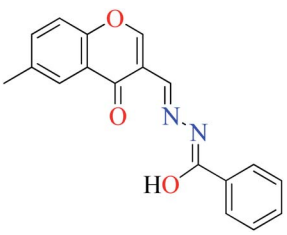	**L8**	240	54[b]
	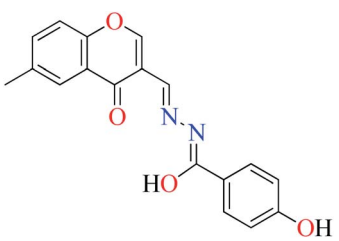	**L9**	230	

Table 1 (*Contd.*)

Entry	Compounds	Structure number	IC_{50} (μM)	Ref.
	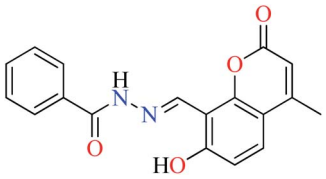	**L10**	Not reported clearly	55[b]
2				53[a]
2a	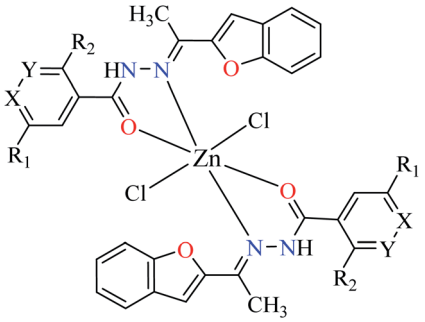			
	1 = $[Zn(\mathbf{L1})_2]Cl_2$	**1** X = N; Y = C; R_1 = H; R_2 = H	101.29	
	2 = $[Zn(\mathbf{L2})_2]Cl_2$	**2** X = C; Y = N; R_1 = H; R_2 = H	56.27	
	3 = $[Zn(\mathbf{L3})_2]Cl_2$	**3** X = C–NO_2; Y = C; R_1 = H; R_2 = H	27.71	
	4 = $[Zn(\mathbf{L4})_2]Cl_2$	**4** X = C; Y = C; R_1 = H; R_2 = NO_2	97.26	
	5 = $[Zn(\mathbf{L5})_2]Cl_2$	**5** X = C; Y = C–NH_2; R_1 = H; R_2 = H	NA	
	6 = $[Zn(\mathbf{L6})_2]Cl_2$	**6** X = C; Y = C; R_1 = Br; R_2 = H	121.19	
2b	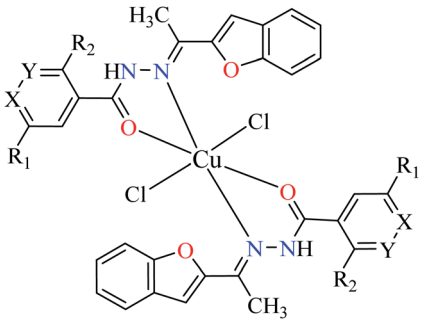			
	9 = $[Cu(\mathbf{L1})_2]Cl_2$	**9** X = N; Y = C; R_1 = H; R_2 = H	>500	
	10 = $[Cu(\mathbf{L2})_2]Cl_2$	**10** X = C; Y = N; R_1 = H; R_2 = H	17.73	
	11 = $[Cu(\mathbf{L3})_2]Cl_2$	**11** X = C–NO_2; Y = C; R_1 = H; R_2 = H	1.15	
	12 = $[Cu(\mathbf{L4})_2]Cl_2$	**12** X = C; Y = C; R_1 = H; R_2 = NO_2	18.91	
	13 = $[Cu(\mathbf{L5})_2]Cl_2$	**13** X = C; Y = C–NH_2; R_1 = H; R_2 = H	0.15	
	14 = $[Cu(\mathbf{L6})_2]Cl_2$	**14** X = C; Y = C; R_1 = Br; R_2 = H	0.21	
	15 = $[Cu(\mathbf{L7})_2]Cl_2$	**15** X = C; Y = C; R_1 = H; R_2 = Cl	NA	
2c	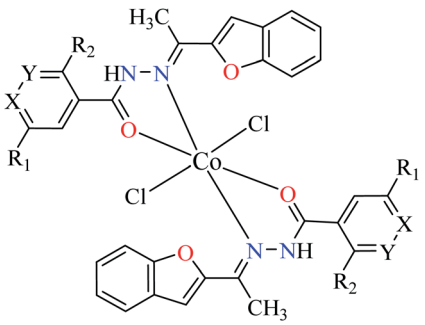			
	22 = $[Co(\mathbf{L1})_2]Cl_2$	**22** X = N; Y = C; R_1 = H; R_2 = H	NA	
	23 = $[Co(\mathbf{L2})_2]Cl_2$	**23** X = C; Y = N; R_1 = H; R_2 = H	66.48	
	24 = $[Co(\mathbf{L3})_2]Cl_2$	**24** X = C–NO_2; Y = C; R_1 = H; R_2 = H	153.23	
	25 = $[Co(\mathbf{L4})_2]Cl_2$	**25** X = C; Y = C; R_1 = H; R_2 = NO_2	96.95	

Table 1 (*Contd.*)

Entry	Compounds	Structure number	IC_{50} (μM)	Ref.
2d	**26** = $[Co(\mathbf{L5})_2]Cl_2$ **27** = $[Co(\mathbf{L6})_2]Cl_2$ **28** = $[Co(\mathbf{L7})_2]Cl_2$ 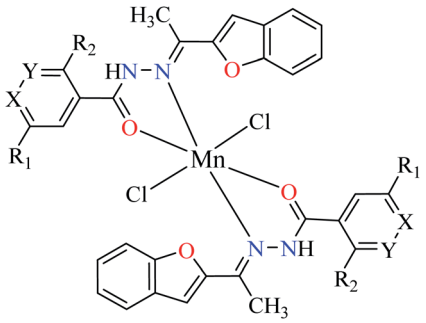	**26** X = C; Y = C–NH_2; R_1 = H; R_2 = H **27** X = C; Y = C; R_1 = Br; R_2 = H **28** X = C; Y = C; R_1 = H; R_2 = Cl	NA 213.30 NA	
3	**30** = $[Mn(\mathbf{L1})_2]Cl_2$ **31** = $[Mn(\mathbf{L2})_2]Cl_2$ **32** = $[Mn(\mathbf{L3})_2]Cl_2$ **33** = $[Mn(\mathbf{L4})_2]Cl_2$ **34** = $[Mn(\mathbf{L5})_2]Cl_2$ **35** = $[Mn(\mathbf{L7})_2]Cl_2$	**30** X = N; Y = C; R_1 = H; R_2 = H **31** X = C; Y = N; R_1 = H; R_2 = H **32** X = C–NO_2; Y = C; R_1 = H; R_2 = H **33** X = C; Y = C; R_1 = H; R_2 = NO_2 **34** X = C; Y = C–NH_2; R_1 = H; R_2 = H **35** X = C; Y = C; R_1 = H; R_2 = Cl	45.63 143.21 345.62 NA NA 457.28	54[b]
3a	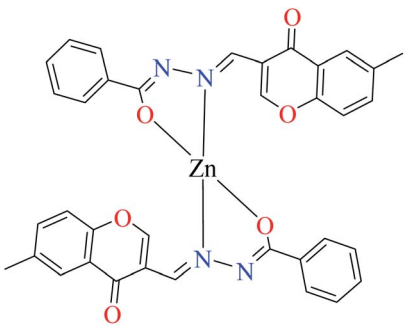 **7** = $[Zn(\mathbf{L8})_2]\cdot 2H_2O$	**7**	180	
3b	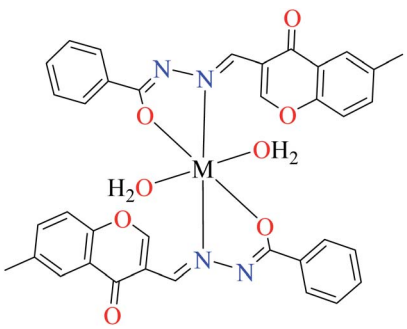 M(II) = Cu, Ni **16** = $[Cu(\mathbf{L8})_2(OH_2)_2]\cdot H_2O$ **19** = $[Ni(\mathbf{L8})_2(OH_2)_2]\cdot H_2O$	**16** **19**	140 200	
3c	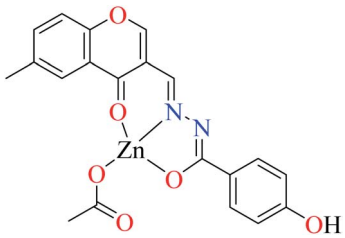			

Table 1 (*Contd.*)

Entry	Compounds	Structure number	IC_{50} (μM)	Ref.
3d	**8** = $[Zn(\mathbf{L9})CH_3COO]\cdot H_2O$ 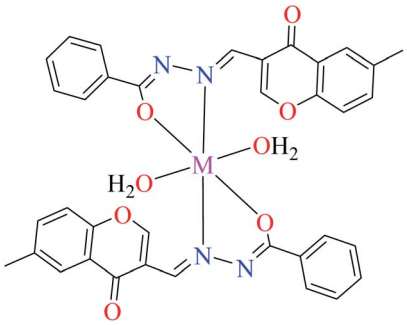 M(II) = Cu, Ni	**8**	190	
	17 = $[Cu(\mathbf{L9})_2(OH_2)_2]\cdot H_2O$	**17**	170	
	20 = $[Ni(\mathbf{L9})_2(OH_2)_2]\cdot H_2O$	**20**	230	
4	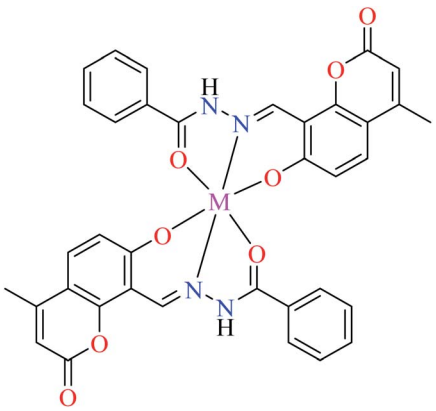 M(II) = Cu, Ni, Co, Mn			55[b]
	18 = $[Cu(\mathbf{L10})_2]$	**18**	Not reported clearly	
	21 = $[Ni(\mathbf{L10})_2]$	**21**	Not reported clearly	
	29 = $[Co(\mathbf{L10})_2]$	**29**	Not reported clearly	
	36 = $[Mn(\mathbf{L10})_2]$	**36**	Not reported clearly	

[a] Acarbose as the reference drug (IC_{50} = 378.25 μM). [b] Acarbose as the reference drug (IC_{50} = 99 μM).

Table 2 α-Glucosidase inhibitory activity of divalent metal complexes bearing picolinic acid (PicAs)

Entry	Compounds	Structure number	IC_{50} (μM)	Ref.
1	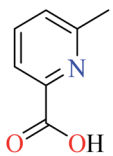	**L11**	NA	62[a]
	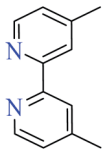	**L12**	NA	62[a]

Table 2 (*Contd.*)

Entry	Compounds	Structure number	IC_{50} (μM)	Ref.
	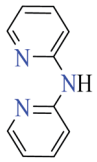	**L13**	NA	63[a]
	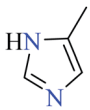	**L14**	NA	63[a]
	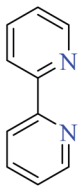	**L15**	NA	67[a]
		**L16**	Not reported	64[a]
	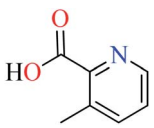	**L17**	NA	68[a]
	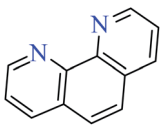	**L18**	NA	68[a]
	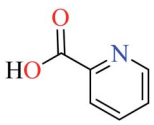	**L19**	NA	65[a]
	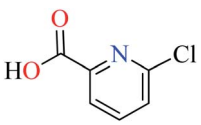	**L20**	NA	65[a]
2				64[a]
2a	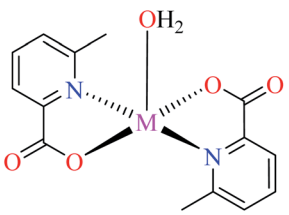			
	M(II) = Zn, Cu			
	37 = [Zn(**L11**)$_2$(H$_2$O)]	**37**	546.04	
	42 = [Cu(**L11**)$_2$(H$_2$O)]	**42**	2.95	

Table 2 (*Contd.*)

Entry	Compounds	Structure number	IC_{50} (μM)	Ref.
2b	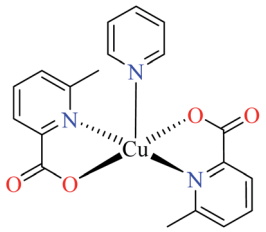			
	43 = [Cu(**L11**)$_2$(**L16**)]	**43**	3.49	
2c	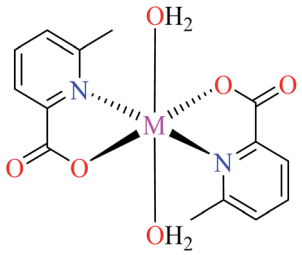			
	M(II) = Ni, Co, Mn			
	48 = [Ni(**L11**)$_2$(H_2O)$_2$]	**48**	>600	
	53 = [Co(**L11**)$_2$(H_2O)$_2$]	**53**	>600	
	61 = [Mn(**L11**)$_2$(H_2O)$_2$]	**61**	>600	
3	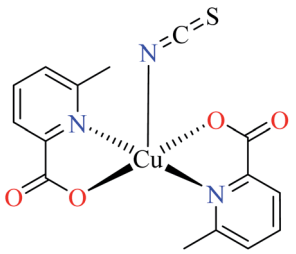			
	44 = [Cu(**L11**)$_2$(NCS)]	**44**	8.02	66[b]
4				67[a]
4a	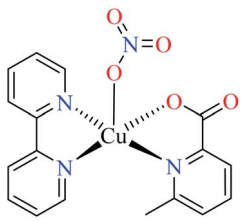			
	45 = [Cu(**L11**)(**L15**)(NO_3)]	**45**	688.94	
4b	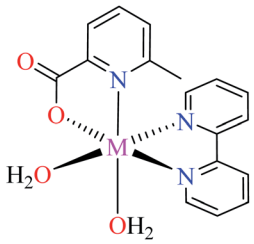			
	M(II) = Ni, Mn			
	49 = [Ni(**L11**)(**L15**)(H_2O)$_2$]	**49**	>600	
	62 = [Mn(**L11**)(**L15**)(H_2O)$_2$]	**62**	>600	

Table 2 (*Contd.*)

Entry	Compounds	Structure number	IC_{50} (μM)	Ref.
4c	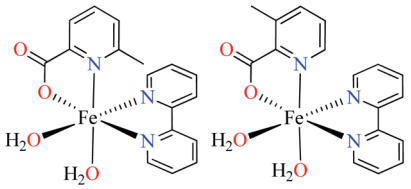			
	59 60			
	59 = [Fe(**L11**)(**L15**)$(H_2O)_2$]	**59**	97.33	
	60 = [Fe(**L17**)(**L15**)$(H_2O)_2$]	**60**	724.25	
4d	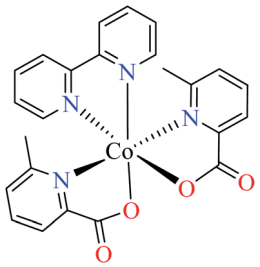			
	54 = [Co(**L11**)$_2$(**L15**)]	**54**	>600	
5	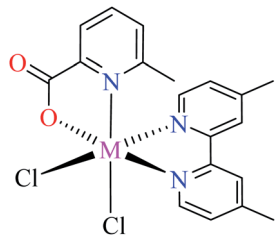			
	M(II) = Zn, Ni			
	38 = [Zn(**L11**)(**L12**)$(Cl)_2$]	**38**	>600	62[a]
	50 = [Ni(**L11**)(**L12**)$(Cl)_2$]	**50**	>600	
6				63[a]
6a	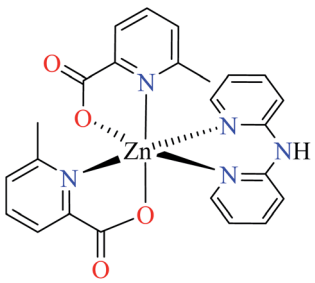			
	39 = [Zn(**L11**)$_2$(**L13**)]	**39**	>600	
6b	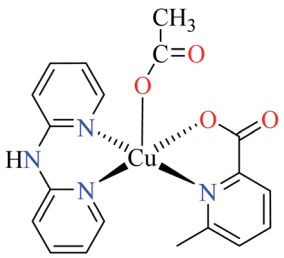			
	46 = [Cu(**L11**)(**L13**)(CH_3COO)]	**46**	513.10	

Table 2 (*Contd.*)

Entry	Compounds	Structure number	IC_{50} (μM)	Ref.
6c	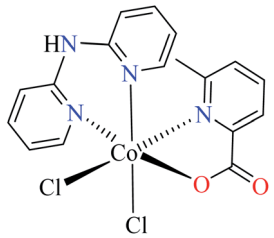			
	55 = [Co(**L11**)(**L13**)$(Cl)_2$]	**55**	>600	
7				63[a]
7a	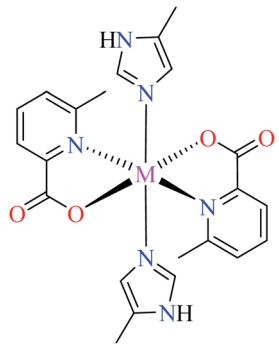			
	M(II) = Zn, Co, Mn			
	40 = [Zn(**L11**)$_2$(**L14**)$_2$]	**40**	>600	
	56 = [Co(**L11**)$_2$(**L14**)$_2$]	**56**	>600	
	63 = [Mn(**L11**)$_2$(**L14**)$_2$]	**63**	>600	
7b	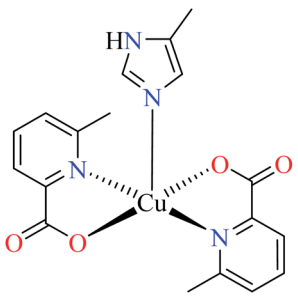			
	47 = [Cu(**L11**)$_2$(**L14**)]	**47**	2.91	
7c	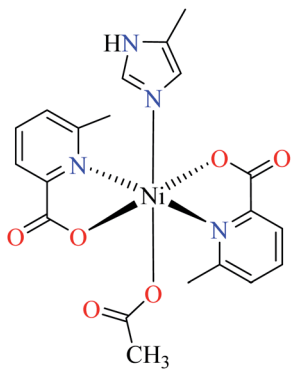			
	51 = [Ni(**L11**)$_2$(**L14**)(CH_3COO)]	**51**	>600	

Table 2 (*Contd.*)

Entry	Compounds	Structure number	IC_{50} (μM)	Ref.
8				68[a]
8a	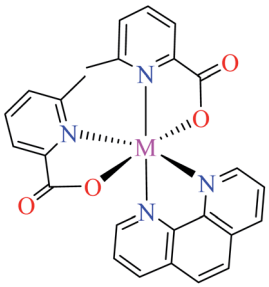			
	M(II) = Ni, Co, Mn			
	52 = [Ni(**L11**)$_2$(**L18**)]	**52**	>600	
	57 = [Co(**L11**)$_2$(**L18**)]	**57**	>600	
	64 = [Mn(**L11**)$_2$(**L18**)]	**64**	>600	
8b	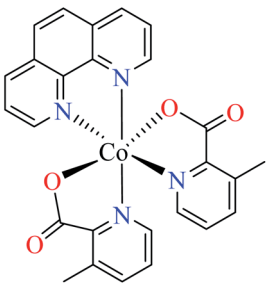			
	58 = [Co(**L17**)$_2$(**L18**)]	**58**	>600	
9	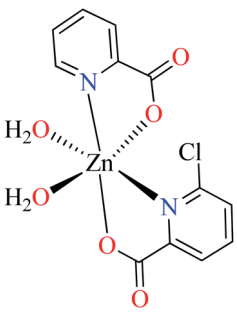			
	41 = [Zn(**L19**)(**L20**)(H_2O)$_2$]	**41**	440	65[a]

[a] Genistein as the reference drug (IC_{50} = 16.57 ± 0.23 μM). [b] Genistein as the reference drug (IC_{50} = 7.85 ± 0.87 μM).

In the same series of ligands, Ni(II) complexes were found to be weaker than those of Zn(II) and Cu(II).

Cobalt(II) complexes. As α-glucosidase inhibitory activity of various metal(II) complexes containing 2-acetylbenzofuran hydrazide moiety was investigated by Khan *et al.*,[53] cobalt(II) complexes, **22–28** (Table 1, entry 2c) were evaluated and found to be more active than the free ligands (**L1–L7**) and moderate inhibitors of the enzyme (IC_{50} = 66.48–153.23 μM). The best activity was related to the complex **23** (IC_{50} = 66.48 μM comparing with acarbose = 378.25 μM) containing **L2** (NA). It should be noted that Zn(II) and Cu(II) complexes of **L2** were more potent than **23**, especially that of Cu(II) which endorses the electronic effect of the metal in the inhibitory activity of complexes with the same geometry (disordered octahedral). Complexes **22**, **26**, and **28** were completely inactive toward enzyme.

Manganese(II) complexes. Evaluation of α-glucosidase inhibitory activity of Mn(II) complexes coordinated with 2-acetylbenzofuran hydrazones **30–35** (Table 1, entry 2d) showed that complex **30** having ligand **L1** was the most potent compound (IC_{50} = 45.63 μM) among Mn(II) complexes (IC_{50} = 45.63–457.28 μM). Free **L1** had no inhibitory activity toward α-glucosidase indicating the efficacy of related complex and the role of metal center (electronic or structural effect) of the complex in the enzyme inhibition. Complexes **33** and **34** depicted no activity in which the metal center could not construct favorable interactions with the enzyme.[53]

Table 3 α-Glucosidase inhibitory activity of divalent metal complexes bearing Schiff base ligands

Entry	Compounds	Structure number	Yeast enzyme IC_{50} (μM)	rat intestinal enzyme IC_{50} (μM)	Ref.
	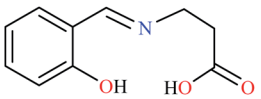	**L21**	NA	NA	
	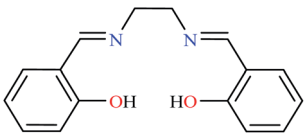	**L22**	NA	NA	
1	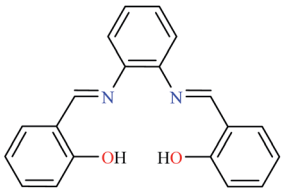	**L23**	NA	NA	72[a]
	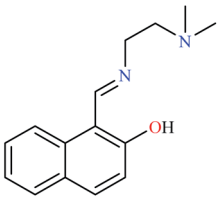	**L24**	NA	NA	
2					72[a]
2a	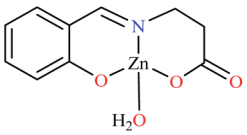				
	65 = [Zn(**L21**)(H_2O)]	**65**	2.89	126.00	
2b					
	66 = [Zn(**L22**)]	**66**	3.10	189.00	
2c	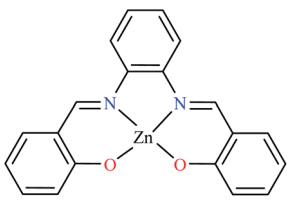				
	67 = [Zn(**L23**)]	**67**	16.10	NA	
2d	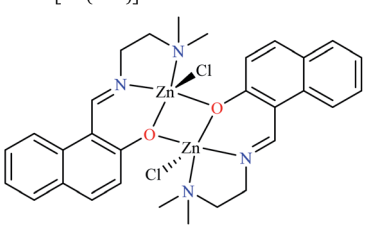				
	68 = [Zn_2(**L24**)$_2$($Cl)_2$]	**68**	4.06	86.0	

[a] Not reported.

Table 4 α-Glucosidase inhibitory activity of divalent metal complexes bearing diamine ligands

Entry	Compounds	Structure number	IC_{50} (mg mL^{-1})	Ref.
1	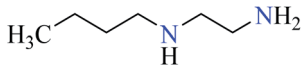	**L25**	Not reported	74[a]
	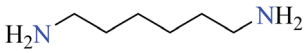	**L26**	Not reported	74[a]
	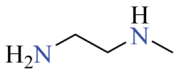	**L27**	Not reported	75[b]
	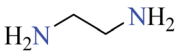	**L28**	Not reported	76[a]
2	$[Zn(\mathbf{L25})_3].2Cl$	**69**	298	74[a]
	$[Zn(\mathbf{L25})_3].2NO_3$	**70**	278	
	$[Zn(\mathbf{L25})_3]\cdot SO_4$	**71**	305	
	$[Cu(\mathbf{L25})_3]\cdot 2Cl$	**78**	266	
	$[Cu(\mathbf{L25})_3]\cdot 2NO_3$	**79**	279	
	$[Cu(\mathbf{L25})_3]\cdot SO_4$	**80**	256	
	$[Ni(\mathbf{L25})_3]\cdot 2Cl$	**87**	226	
	$[Ni(\mathbf{L25})_3]\cdot 2NO_3$	**88**	198	
	$[Ni(\mathbf{L25})_3]\cdot SO_4$	**89**	218	
3	$[Zn(\mathbf{L26})_3]\cdot 2Cl$	**72**	1.19	74[a]
	$[Zn(\mathbf{L26})_3]\cdot 2NO_3$	**73**	1.50	
	$[Zn(\mathbf{L26})_3]\cdot SO_4$	**74**	1.43	
	$[Cu(\mathbf{L26})_3]\cdot 2Cl$	**81**	1.33	
	$[Cu(\mathbf{L26})_3]\cdot 2NO_3$	**82**	1.26	
	$[Cu(\mathbf{L26})_3]\cdot SO_4$	**83**	1.76	
	$[Ni(\mathbf{L26})_3]\cdot 2Cl$	**90**	3.63	
	$[Ni(\mathbf{L26})_3]\cdot 2NO_3$	**91**	2.70	
	$[Ni(\mathbf{L26})_3]\cdot SO_4$	**92**	2.00	
	$[Co(\mathbf{L26})_3]\cdot Cl_2$	**96**	1348	
	$[Co(\mathbf{L26})_3]\cdot (NO_3)_2$	**97**	1279	
	$[Co(\mathbf{L26})_3]\cdot SO_4$	**98**	1198	
4	$[Zn(\mathbf{L27})_3]\cdot 2Cl$	**75**	2.13	75[b]
	$[Zn(\mathbf{L27})_3]\cdot 2NO_3$	**76**	1.05	
	$[Zn(\mathbf{L27})_3]\cdot SO_4$	**77**	2.0	
	$[Ni(\mathbf{L27})_3]\cdot 2Cl$	**93**	2.53	
	$[Ni(\mathbf{L27})_3]\cdot 2NO_3$	**94**	1.74	
	$[Ni(\mathbf{L27})_3]\cdot SO_4$	**95**	1.93	
	$[Co(\mathbf{L27})_3]\cdot Cl_2$	**99**	1.20	
	$[Co(\mathbf{L27})_3]\cdot (NO_3)_2$	**100**	0.90	
	$[Co(\mathbf{L27})_3]\cdot SO_4$	**101**	1.09	
5	$[Cu(\mathbf{L28})_3]\cdot 2Cl$	**84**	0.80	76[a]
	$[Cu(\mathbf{L28})_3]\cdot 2NO_3$	**85**	0.47	
	$[Cu(\mathbf{L28})_3]\cdot SO_4$	**86**	0.61	

[a] Acarbose as the reference drug (IC_{50} = 0.140 mg mL^{-1}). [b] Acarbose as the reference drug (IC_{50} = 0.143 mg mL^{-1}).

Picolinic acids metal(II) complexes

Picolinic acid (PicA) known as the tryptophan metabolite has a low toxicity to mammals. Oral administration of PicA helps the absorption of several metal ions through the small intestine.[56–58] This compound which is an isomer of nicotinic acid and isonicotinic acid is a chelating agent for metals such as chromium, zinc, manganese, copper, iron and molybdenum in the human body.[59] Most of its complexes are lipophilic, so PicA can play an important role in the absorption of metals such as zinc in the human body.[60] Because different applications of picolinic acid derivatives (PicAs) such as catalysis, ion exchange, nonlinear optics and physicochemical properties are used for the synthesis of different structures containing coordination complexes. Therefore, this compound is very widely used in the field of bio-inorganic chemistry.

PicA complex of copper(II) has demonstrated very potent *in vitro* anti-α-glucosidase activity (IC_{50} = 1.28 μM) comparing with acarbose (IC_{50} = 747 μM). It was also evaluated *in vivo* and could inhibit the α-glucosidase action in ddy mice after oral administration of sucrose and the blood glucose levels were remarkably suppressed. However, it could not change the blood glucose levels in mice administered with glucose.[61]

6-Methylpicolinic acid (**L11**) and 3-methylpicolinic acid (**L17**) was found to be inactive toward α-glucosidase, however, the coordinated products showed proper activity (Table 2) to

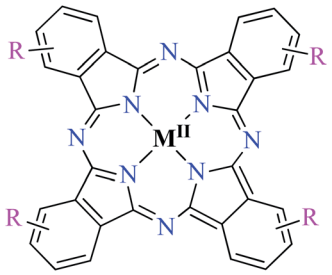

M^{II} = Zn, Cu, Ni, Co, Mn

Zn(II) complexes: **138**: Zn(**L60**), **139**: Zn(**L62**), **140**: Zn(**L63**), **141**: Zn(**L64**), **142**: Zn(**L65**), **143**: Zn(**L66**), **144**: Zn(**L72**), **145**: Zn(**L67**)

Cu(II) complexes: **146**: Cu(**L60**), **147**: Cu(**L64**), **148**: Cu(**L72**), **149**: Cu(**L61**), **150**: Cu(**L68**), **151**: Cu(**L69**)

Ni(II) complexes: **152**: Ni(**L64**), **153**: Ni(**L61**), **154**: Ni(**L73**)

Co(II) complexes: **156**: Co(**L72**), **157**: Co(**L67**), **158**: Co(**L68**), **159**: Co(**L69**), **160**: Co(**L70**), **161**: Co(**L71**), **162**: Co(**L73**), **163**: Co(**L74**)

Mn(II) complexes: **164**: Mn(**L60**), **165**: Mn(**L64**), **166**: Mn(**L70**), **167**: Mn(**L71**), **168**: Mn(**L73**)

Fig. 3 The structure of phthalocyanine complexes with Zn(II), Cu(II), Ni(II), Co(II), and Mn(II) ions. Phthalocyanine ligands L60–L74 were demonstrated in Table 7.

confirm desired role of metal(II) ions in the enzyme inhibitory activity.

Zinc(II) complexes. Avcı *et al.* recently reported various Zn(II) complexes containing 6-methylpyridine-2-carboxylic (**L11**) as α-glucosidase inhibitors (**37–40**, Table 2, entries 2a, 5, 6a, and 7a).[62–64]

Complex **37**[64] possessing a square pyramidal geometry, contained two bidentate **L11** ligands and depicted low inhibitory activity (IC_{50} > 546 μM) compared with genistein (IC_{50} = 16.57 μM). However, replacement of one of **L11** by 4,4′-dimethyl-2,2′-bipyridyl (**L12**),[62] 2,2′-dipyridylamine (**L13**),[63] and 4(5) methylimidazole (**L14**)[63] to form complexes **38–40** having distorted octahedral geometry (Table 2, entries 5, 6a, and 7a), could not improve the IC_{50} values (IC_{50} > 600 μM). Moreover, Dege *et al.* have synthesized a novel Zn(II) complex having 2-picolinic acid (**L19**) and 6-chloropicolinic acid (**L20**) ligands with distorted octahedral geometry (Table 2, entry 1) and examined the inhibitory activity of the complex (**41**, Table 2, entry 9),[65] comparing with genistein as a reference drug (IC_{50} = 8 μM). Comparing of the inhibitory activity of complex **37** (IC_{50} = 546.04 μM) with **41** (IC_{50} = 440 μM) revealed that the replacement of methyl group with Cl did not lead to significant inhibitory activity. In general, the low activity of Zn(II) complexes containing PicA moiety can be associated with the full d orbitals of metal center ion. It should be mentioned that all ligands (**L11–L20**) were also inactive toward α-glucosidase.

Copper(II) complexes. Avcı *et al.* also evaluated inhibitory properties of a series of Cu(II) complexes (**42–47**, Table 2, entries 2a, 2b, 3, 4a, 6b and 7b) possessing **L11** (Table 2, entry 1) with distorted trigonal bipyramidal structure, against α-glucosidase.[62–64,66,67] Among them, complexes **42**[64] and **47**[63] showed the best activity with IC_{50} values of 2.95 and 2.91 μM, respectively. Good results may be associated with the ability of water and imidazole (**L14**) in the construction of H-bonding interaction with the enzyme.

In complex **43**,[64] the third ligand, water was replaced by the pyridine (**L16**, Table 2, entry 1) which led to the reduction of activity from IC_{50} = 2.95 μM to 3.49 μM compared with genistein (IC_{50} = 16.57 μM). That was associated with the π-conjugation effect of **L16**. Comparison of the activity of complex **42** with its counterpart, complex **37**, indicated the essential role of Cu^{2+} ions as the metal center in the α-glucosidase inhibitory activity.

Although the introduction of isothiocyanate into the Cu(II) complex **44** afforded the inhibitory potency (IC_{50} = 8.02 μM) approximately as potent as the genistein (IC_{50} = 7.85 μM), it was not as efficient as water and pyridine (**42** and **43**, respectively).[66]

The efficacy of other complexes containing mixed-ligands **45**[67] (IC_{50} = 688.94 μM) and **46** (IC_{50} = 513.10 μM)[63] has been also investigated. The presence of 2,2′-bipyridyl (**L15**) and nitrate in complex **45** and 2,2′-dipyridylamine (**L13**) and acetate in complex **46**, reduced the inhibitory activity compared with **42**, **43**, **44**, and **47** in spite of the same geometry.

Distinguished α-glucosidase inhibitory activity of Cu(II) complexes of PicAs **42–47** compared with non-active free ligands can be explained from various points of view. The structural and electronic role of Cu(II) ion in providing desired binding affinity toward the enzyme, is significant.

Nickel(II) complexes. As studied by Avcı *et al.*, Ni(II) complexes of **L11** with distorted octahedral geometry (**48–52**, Table 2, entries 2c, 4b, 5, 7c and 8a) were not active toward α-glucosidase (IC_{50} > 600 μM, comparing with genistein (IC_{50} = 16.57 μM)).[62–64,67,68] It seems that Ni(II) complexes could not establish appropriate structural and electronic properties for the inhibition of enzyme as changing the number and nature of coordinated ligands did not afford anti-α-glucosidase activity.

Cobalt(II) complexes. Anti-α-glucosidase activity of various Co(II) complexes (**53–58**, Table 2, entries 2c, 4d, 6c, 7a, 8a, and 8b) containing 6-methylpicolinic acid (**L11**) and 3-methylpicolinic acid (**L17**) (Table 2, entry 1) was reported by Avcı *et al.*[62–64,67,68] All complexes **53–58** were inactive toward α-glucosidase (IC_{50} > 600 μM). Introduction of different ligands such as water (complex **53**, Table 2, entry 2c), 2,2′-bipyridyl (**L15**, Table 2, entry 1, complex **54**, Table 2, entry 4d), chlorine (complex **55**, Table 2, entry 6c), 2,2′-dipyridylamine (**L13**, Table 2, entry 1, complex **55**, Table 2, entry 6c), and imidazole (**L14**, Table 2, entry 1, complex **56**, Table 2, entry 7a) as well as changing the position of methyl group on the PicA moiety (**57** and **58**, Table 2, entries 8a and 8b)[68] did not affect the inhibitory activity.

Iron(II) complexes. Anti-α-glucosidase activity of Fe(II) complexes has not been widely reported in the literature and two complexes **59** and **60** (Table 2, entry 4c) based on the **L11** and **L17** containing **L15** were studied by Avcı *et al.*[67] Complexes **59** containing 6-methylpicolinic acid (**L11**) showed IC_{50} value of 97.33 μM comparing with genistein (IC_{50} = 16.57 μM). Changing the position of methyl group from 6- to 3- of PicA moiety led to a 7-fold reduction of activity (IC_{50} = 724.25 μM).

Comparison of Fe(II) complexes with their counterparts **57** and **58** demonstrated that the position of methyl group on PicA

moiety played an important role in inhibitory activity, however, it was not found to be important for **57** and **58**. It may be related to the more significant electronic property of Fe(II) than that of Co(II) in spite of same geometry of distorted octahedral.

Manganese(II) complexes. Evaluation of α-glucosidase inhibitory properties of Mn(II) complexes bearing **L11** (**61–64**, Table 2, entries 2c, 4b, 7a, and 8a) was reported by Avcı *et al.*[62–64,67,68] All complexes lacked inhibitory activity (IC_{50} > 600 μM) indicating that Mn(II) similar to Co(II) and Ni(II), could not provide desired electronic and structural properties.

Schiff bases metal(II) complexes

Schiff bases are the popular organic ligands in the coordination chemistry possessing significant role in the induction of different biological activities. It was found that Schiff base complexes especially those having tetrahedral or octahedral geometry, have demonstrated DNA-binding properties and DNA-cleavage activities,[69] antifungal, antibacterial, antimalarial, anti-proliferative and anticancer, anti-inflammatory, antiviral, and antipyretic activity.[70,71] The imine nitrogen is basic and exhibits pi-acceptor properties. Most of the biological properties of these compounds are due to their pi-acceptor properties. Schiff bases are commonly bi- or tri-dentate ligands, able to form stable complexes with transition metals. Schiff base reactions are important for the formation of nitrogen–carbon double bonds in organic chemistry. Also, they are used as liquid crystals.[70]

Zinc(II) complexes. Miyazaki *et al.* investigated *in vitro* inhibitory potency of four Schiff base complexes of Zn(II) **65–68** (Table 3, entry 2) toward yeast and rat intestinal α-glucosidase.[72] They contained Schiff base moiety including *N*-salicylidene-β-alanine (**L21**), *N*–*N*′-bis(salicylidene)ethylenediamine (**L22**), *N*,*N*′-bis(salicylidene)-phenylenediamine (**L23**), and 1-[(2-dimethylaminoethylimino)methyl]naphtholate (**L24**) (Table 3, entry 1). **L21–L24** showed no inhibitory activity on both enzymes, however, related complexes showed potent activity especially on yeast type. Complexes were generally showed more activity on yeast enzyme than rat intestinal type. Compound **65** having *N*-salicylidene-β-alanine moiety revealed the best activity on yeast α-glucosidase with IC_{50} value of 2.89 μM and the activity was reduced toward rat intestinal α-glucosidase as the corresponding IC_{50} value was obtained as 126.00 μM. Complex **68** possessing 1-[(2-dimethylaminoethylimino)methyl]naphtholate showed good activity toward both enzyme types (IC_{50}s = 4.06 and 86.0 μM), respectively (Table 3, entry 2d), and selected for the *in vivo* test to evaluate oral maltose and glucose tolerance as well as the mode of α-glucosidase inhibition. The results indicated that the post-prandial blood glucose levels were reduced using the complex **68** as compared to the control group. It should be noted that **L24** that was non-active in *in vitro* studies, it exhibited an anti-hyperglycemic effect in the glucose-loading test.

Diamines metal(II) complexes

Diamines are organic compounds with two groups of amino groups. The term diamine refers to type-I diamines because of the high reactivity of the first type of amines. They are used as monomers to produce polyimides and polyureas. 1,2-Diamine derivatives are the most practical moieties in the structure of biological compounds and coordination chemistry.[73] Many natural products that have significant biological properties contain at least one 1,2-diamino component in their structure. Also, complexes of 1,2-diamino groups have been widely investigated for their biological properties. For example, 1,2-diamino complexes of Pt(II) demonstrated more antitumor activity than cisplatin due to lower toxicity and drug resistance.[73]

Four types of diamines including *N*-(*n*-butyl) ethylenediamine (**L25**),[74] 1,6-diaminohexane (**L26**),[74] *N*-methylethylenediamine (**L27**),[75] and ethylenediamine (**L28**)[76] were used and the effect of the counterion (chloride, nitrate, and sulphate) was also considered in this series. As can be seen in Table 4, Cu(II) complexes of ethylenediamine (**L28**) possessed much higher activity than Zn(II), Ni(II), and Co(II).

Zinc(II) complexes. α-Glucosidase inhibitory activity of a series of Zn(II) complexes bearing diamines (**69–77**, Table 4, entries 2, 3, and 4) was studied by Tripathi *et al.*[74,75] comparing with acarbose (IC_{50} = 0.14 mg mL^{-1}). Among them, Zn(II) complexes of **L25** showed lower activity (IC_{50} = 278–305 mg mL^{-1}) than those of **L26** (IC_{50} = 1.19–1.50 mg mL^{-1}) and **L27** (IC_{50} = 1.05–2.13 mg mL^{-1}). Also, the presence of nitrate as the counterion was found to be appropriate for improving inhibitory activity in the series of Zn(II) complexes (**70**, **73**, and **76**).

Copper(II) complexes. In the series of Cu(II) complexes (**78–86**, Table 4, entries 2, 3, and 5),[74,76] similar to Zn(II) complexes, complexes of **L25** (**77–79**, IC_{50} = 256–279 mg mL^{-1}) exhibited lower activity than those of **L26** (IC_{50} = 1.26–1.76 mg mL^{-1}) and **L28** (IC_{50} = 0.47–0.80 mg mL^{-1}). Taken together, the efficacy of ethylenediamine **L28** (complexes **84–86**) was more significant than 1,6-diaminohexane **L26** (complexes **81–83**). Also, the presence of nitrate ions (NO_3^-) was found to be generally proper.

Nickel(II) complexes. Ni(II) complexes (**87–95**, Table 4, entries 2, 3, and 4)[74,75] were synthesized by Tripathi *et al.* Results obtained from *in vitro* inhibitory studies confirmed that **L25** was not desired ligand coordinated to the metal center for the induction of potent α-glucosidase inhibitory activity (IC_{50} = 198–226 mg mL^{-1}) as compared with **L26** (IC_{50} = 2.00–3.63 mg mL^{-1}) and **L27** (IC_{50} = 1.74–2.53 mg mL^{-1}). However, comparison of complexes of **L26** and **L27** counterparts, indicated higher efficacy of **L27** than **L26**. Also, difference of counterions did not play a regular role in the inhibitory activity.

Cobalt(II) complexes. Co(II) complexes reported by Tripathi *et al.*, were synthesized using **L26** (**96–98**, Table 4, entry 3) and **L27** (**99–101**, Table 4, entry 4). The inhibitory activity of **L27** complexes was much higher (IC_{50} = 0.9–1.20 mg mL^{-1})[75] than **L26** counterparts (IC_{50} = 1198–1348 mg mL^{-1}).[74]

Trivalent metal complexes as α-glucosidase inhibitors

The activity of trivalent transition metal complexes as α-glucosidase inhibitors is not well understood and a few studies have

been reported in this field. All known modes of life need iron. Among iron compounds, iron(III) ion is usually the most stable species in the air, as demonstrated by the pervasiveness of rust, an unsolved iron(III)-containing material. Iron(III) is a d^5 center, indicating that the iron(III) has five valence electrons in the 3d orbital shell. These d-orbitals can accept a large variety of ligands to form coordination complexes. Normally, ferric ions are enclosed by six ligands arranged in octahedral; but sometimes three and sometimes as many as seven ligands are seen.[77] Many proteins in existing beings contain fixed iron(III) ions which are important subclass of the metalloproteins including oxyhemoglobin, ferredoxin, and cytochromes.[78]

Chromium especially Cr(III) is an important bioelement for the mammalian organism.[79] It plays an essential role in the maintenance of a normal glucose tolerance to maintain regular carbohydrate and lipid metabolism.[80,81] The direct relation between chromium deficiency and glucose intolerance has been clinically studied.[82] Cr(III) glycinate complex has also been reported to improve blood glucose levels and reduces the copper to zinc ratio in tissues of rats with mild hyperglycaemia.[83]

Metals(III) are able to form complexes possessing unique properties due to strong interactions with nitrogen-giving and oxygenating ligands resulting in versatile electronic structure and electron density of the complex. For this purpose, study of their biological activities such as α-glucosidase inhibitory activity was considered.

Considering the fact that all ligands **L11**, **L12**, **L17** (Table 2, entry 1) and **L29–L32** (Table 5, entry 1) used for the preparation of trivalent metal complexes are not active toward α-glucosidase, inhibitory activity of resulted complexes is valuable.

Picolinic acid metal(III) complexes

In this part, Fe(III) and Cr(III) complexes containing picolinic acid (PicA) were considered.

Iron(III) complexes. Avcı *et al.* reported anti-α-glucosidase activity two Fe(III) complexes (**102**[64] and **103**,[62] Table 5, entries 2 and 3) having three 6-methylpicolinic acid ligand (**L11**, Table 2, entry 1) and 4,4′-dimethyl-2,2′-bipyridyl (**L12**, Table 2, entry 1) with a distorted octahedral geometry. The IC_{50} values of complexes were calculated as 446.2 and 492.3 μM, respectively, compared with genistein (IC_{50} = 16.575 μM). They were found to be weak inhibitors of α-glucosidase. Complex **102** having three **L11** showed a little better activity than **103** which lacked one of **L11** replacing by electron withdrawing nitrate (NO_3) group. It seems that appropriate interactions with the enzyme were reduced **103**.[62]

Chromium(III) complexes. Avcı *et al.* synthesized and evaluated two distorted octahedral complexes of Cr(III) **104** having 3-methylpicolinic acid **L17** (Table 5, entry 4),[84] and **105** having 6-methylpicolinic acid **L11** (Table 5, entry 5),[66] for their α-glucosidase inhibitory activity and compared with genistein (IC_{50} = 16.575 μM). It should be considered that complex **105** also coordinated to water and isothiocyanate ligands, however, both **104** and **105** showed no inhibitory activity (IC_{50} > 600 μM). Increase of the number of water as a ligand in the complex **106** (Table 5, entry 6),[64] with similar geometry led to higher inhibitory activity (IC_{50} = 164.87 μM)[62] which is probably related to the formation of H-bonding interaction of water with the enzyme.

Hydroxamic acid chromium(III) complexes

Hassan *et al.* reported α-glucosidase inhibitory activity of Cr(III) complexes **107–110** (Table 5, entry 7) of hydroxamic acid derivatives **L29–L32** (Table 5, entry 1) comparing with acarbose as the standard drug (IC_{50} = 418 μM).[85] The efficacy of hydroxamic acid derivatives (**L29–L32**) were found to be more effective than PicAs (**L11**, **L12**, and **L17**), in spite the fact that all ligands were not inhibitor of α-glucosidase. Also, the presence of various substituents on hydroxamic acid moiety played an important role in the inhibitory activity. Among **107–110**, the best activity was reported by complex **107** (IC_{50} = 28.7 μM) with no substituent on the aryl moiety. Introduction of other substituents including CH_3 (**108**), Cl (**110**), and CH_3O (**109**) into the 4-position of the aryl group deteriorated anti-α-glucosidase activity. However, the order of activity was found as CH_3 (IC_{50} = 69.28 μM) > Cl (IC_{50} = 169.5 μM) > OCH_3 (IC_{50} = 355.9 μM).

Tetravalent metal complexes as α-glucosidase inhibitors

Considering the fact that the stability of central metal of the complexes in the high oxidation state is difficult, they have been generally found in polyoxo materials. Among the first row transition metals, vanadium and oxo-vanadium complexes have been frequently synthesized and investigated for their biological properties such as anti-α-glucosidase activity.

Vanadium in the oxidation states III, IV, and V readily forms V=O bond and can coordinate to N and S of small molecules to form stable complexes. The redox potential of V(V) to V(IV) or V(IV) to V(III) have made vanadium a versatile metal in the biological and medicinal applications.[86–90] Under *in vitro* conditions, vanadium compounds stimulate glucose uptake and inhibit lipid breakdown, in a way remarkably suggestive of insulin's effects. Under *in vivo* conditions, vanadium improves insulin's plasma glucose and lipid-lowering properties, leading to normalization of diabetic symptoms in the presence of only minimal endogenous insulin.[87]

Discovery of the insulin-mimetic effect of vanadium ions and their complexes as potential agents for the treatment or opposition of DM has been the most remarkable improvement in the treatment of the disease in the last decade of the 20th century.[39] Subsequently, the effect of vanadyl sulfate ($VOSO_4$) was clinically tested to treat T2DM in the USA since 1995.[91,92]

Vanadium complexes containing O-coordinating atoms are known for their high hydrolytic stability; however, they have shown low redox stability. In this respect, vanadium complexes coordinated to both O- and N-atoms are known for their high hydrolytic stability.[93] Accordingly, complexes of hydrazides, PicAs, and Schiff bases can be versatile candidates for desired α-glucosidase inhibitory activity (Table 6).

Patel *et al.* synthesized mononuclear vanadium(IV) complex (**111**, Table 6, entry 2) of *N*′-[(*E*)-phenyl(pyridin-2-yl) methylidene]benzohydrazide (**L33**) and benzhydrazide (**L34**)

Table 5 α-Glucosidase inhibitory activity of trivalent metal complexes bearing picolinic acid (PicAs) and hydroxamic acid

Entry	Compounds	Structure number	IC_{50} (μM)	Ref.
1	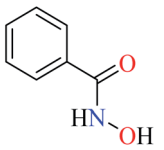	**L29**	NA	85[a]
	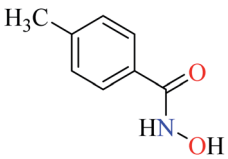	**L30**	NA	
	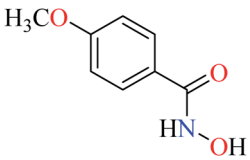	**L31**	NA	
	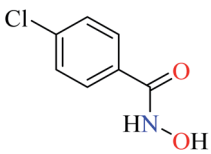	**L32**	NA	
2	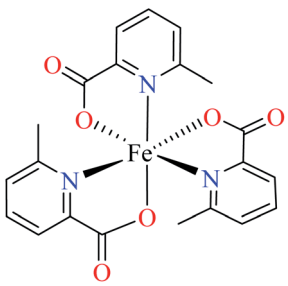			64[b]
	102 = [Fe(**L11**)$_3$]	**102**	446.2	
3	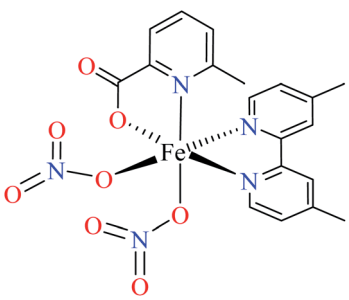			
	103 = [Fe(**L11**)(**L12**)$(NO_3)_2$]	**103**	492.3	62[b]
4	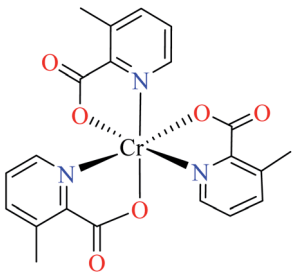			84[b]
	104 = [Cr(**L17**)$_3$]	**104**	>600	

Table 5 (*Contd.*)

Entry	Compounds	Structure number	IC_{50} (μM)	Ref.
5	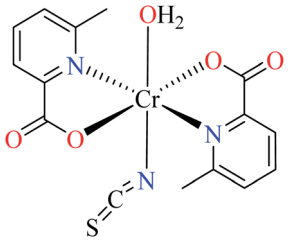			66[c]
	105 = $[Cr(\mathbf{L11})_2(NCS)(H_2O)]$	**105**	>600	
6	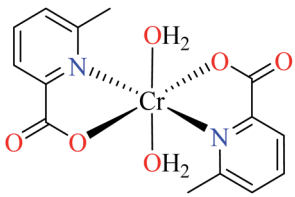			64[b]
	106 = $[Cr(\mathbf{L11})_2(H_2O)_2]$	**106**	164.87	
7	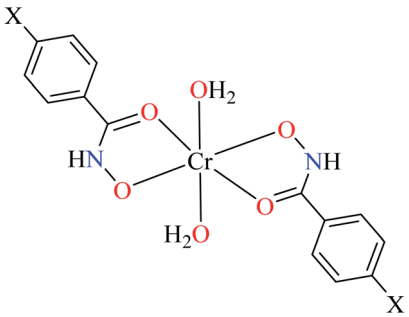			85[a]
	107 = $[Cr(\mathbf{L29})_2(H_2O)_2]$	**107**	28.7	
	108 = $[Cr(\mathbf{L30})_2(H_2O)_2]$	**108**	69.28	
	109 = $[Cr(\mathbf{L31})_2(H_2O)_2]$	**109**	355.9	
	110 = $[Cr(\mathbf{L32})_2(H_2O)_2]$	**110**	169.5	

[a] Acarbose as the reference drug ($IC_{50} = 418 \pm 0.55$ μM). [b] Genistein as the reference drug ($IC_{50} = 16.57 \pm 0.23$ μM). [c] Genistein as the reference drug ($IC_{50} = 7.85 \pm 0.87$ μM).

(Table 6, entry 1)[94] to evaluate its anti-α-glucosidase activity comparing with acarbose (IC_{50} = 18.59 μM). Complex **111** showed good inhibitory activity with IC_{50} value of 14.75 μM.

Ashiq *et al.* prepared various hydrazide vanadium(IV) complexes **112** (Table 6, entry 3a) using 2-phenylacetohydrazide (**L35**) and complexes **113–121** (Table 6, entry 3b) using benzylidenehydrazine derivatives (**L36–L44**).[93] The complex **112** showed very good inhibitory activity ($IC_{50} = 10.7$ μM) comparing with acarbose ($IC_{50} = 780$ μM) and deoxynojirimycin ($IC_{50} = 426$ μM) in spite of lacking activity of **L35**. The inhibitory activity of complexes **113–121** (IC_{50} = 0.68–800 μM) was completely depended on the electronic property of substituents on the aryl ring, as compared with acarbose (IC_{50} = 780 μM) and deoxynojirimycin (IC_{50} = 426 μM). Complex **115** possessing strong electron-releasing methoxy group at 3-position of aryl ring, showed the best activity. Changing the position of methoxy group (complex **119**) led to the reduction of activity (IC_{50} = 38 μM). However, similar trend was observed in the case of complexes **116** and **121** having a strong electron-releasing group (NH_2). Complex **116** having the group at *meta* position of aryl ring showed better activity (IC_{50} = 12.5 μM) than complex **121** possessing the amino group at *para* position (IC_{50} = 16.4 μM). However, the efficacy of amino group at 3-position was lower than the methoxy group by comparing the IC_{50} values of complexes **115** and **116**. However, comparing those of complexes **119** and **121** gave inverse result.

Introduction of a strong electron-withdrawing group (NO_2) into the *meta* opposition of aryl moiety **113** led to much lower activity ($IC_{50} = 67.0$ μM) than those complexes having a strong electron-releasing group (**115**, **116**, **119**, and **121**). Moreover, insertion of halogens (Cl, Br, and I) into the *meat* and *para* position of aryl group (complexes **120**, **114**, **117**, and **118**) gave interesting results. Among halogenated derivatives, **120** having Cl at *para* position of aryl ring was found to be the most active compound (IC_{50} = 13.5 μM). It also was more potent than its counterparts, complexes **119** and **121**. The presence of Br at

meta position of aryl ring (complex **114**) led to relatively good activity (IC_{50} = 20.1 μM). Complexes **117** (IC_{50} = 800 μM) and **118** (IC_{50} = 758 μM) having iodine at 3- or 4-position of the aryl ring demonstrated very low activity which may be related to the steric hindrance of iodine. In the case of complex **120**, electron-donating property of Cl *via* resonance may be important to increase the electron density at central metal inducing desired inhibitory potential.

Picolinic acid vanadium(IV) complexes

Avcı *et al.* synthesized vanadyl complexes **122** (Table 6, entry 4)[62] and **123** (Table 6, entry 5)[84] for their α-glucosidase inhibitory activity comparing with genistein (IC_{50} = 16.57 μM). Complex **122** coordinated to 6-methylpicolinic acid (**L11**, Table 2, entry 1) and 4,4-dimethyl-2,2-bipyridyl (**L12**, Table 2, entry 1). In complex **123**, two ligands were replaced by two 3-methylpicolinic acid ligands (**L17**). Both complexes have distorted square pyramidal structure and showed no activity. It worth mentioning that theoretical calculations from frontier molecular orbitals (FMO) revealed high reactivity and polarizability of complexes **122** and **123**. In addition, the molecular electrostatic potential (MEP) surface indicated high electrophilic and nucleophilic reactivity of both complexes.

Schiff base vanadium(IV) complexes

Rahiman *et al.* synthesized various oxovanadium(IV) complexes (**124–129**, Table 6, entry 6) using 2-(6-methoxynaphthalen-2-yl) propanoic acid (**L45**) and 2-(1-ethylidene)hydrazinecarbothioamide derivatives (**L46–51**).[95] However, ambiguous results in IC_{50} values which were calculated as (%) prevented us to discuss in details. Misra *et al.* synthesized and evaluated oxovanadium(IV) complexes of salicylaldehyde Schiff bases **L52–59** (Table 6, entry 1, complexes **130–137**, Table 6, entry 7) toward rat intestinal α-glucosidase.[96] **L56–59** possessed Br on the aryl ring of salicylaldehyde. **L55**, **L58**, and **L59** showed inhibitory activity with IC_{50} values of 22.72, 74.11, 245.0 μM, respectively, comparing with acarbose (IC_{50} = 18.59 μM). All complexes showed very good anti-α-glucosidase activity, however, those lacking Br on the salicylaldehyde moiety (**130–133**) showed better activity (IC_{50} = 1.26–13.12 μM) than brominated derivatives (**134–137**, IC_{50} = 16.92–62.43 μM). The best activity was obtained by complexes **132** and **133** (IC_{50} = 1.26 μM) which possessed strong electron-donating and electron-withdrawing groups, OMe and NO_2, respectively. The presence of Cl (**131**) at the same position reduced activity and the absence of substituent on the aryl moiety (**130**) was found to be 6 times more potent than **131**. In the case of brominated compounds (**134–137**), complex **136** as the counterpart of **132**, was the weakest inhibitor. Totally, each brominated derivative showed lower activity than counterpart lacking Br, which may be related to the halogen size interrupting the complex from appropriate interactions with the enzyme. In this study,[96] complexe **132** was candidate for the *in vivo* evaluation and it could decrease the blood glucose levels by approximately 12%. However, the corresponding value for acarbose was reported as 35%. The lower activity of **132** in *in vivo* conditions may be related to dissociation of the complex due to low pH inside the intestine.

Phthalocyanine metal complexes

In this review, anti-α-glucosidase activity of complexes of the first-row transition metals including Zn^{2+}, Cu^{2+}, Ni^{2+}, Co^{2+}, Fe^{2+}, Mn^{2+}, Fe^{3+}, Cr^{3+}, and V^{4+} complexes with small molecules; hydrazide, PicAs, Schiff bases, diamines, and hydroxamic acid was discussed. However, macromolecules such as phthalocyanines have been found as the versatile ligands for the formation of desired complexes with first-row transition metals possessing significant α-glucosidase inhibitory properties.

Phthalocyanines and their metal complexes which are structurally related to porphyrin metal complexes, have been widely investigated as chemical sensors,[97] liquid crystals,[98] Langmuir Blodgett films,[99] photovoltaic cells,[100,101] electrochromic materials,[101] optical and electrical materials, catalysts,[102] and photosensitizers in the photodynamic cancer therapy.[103] Also, their enzyme inhibitory activity have been in the center of attention.[104,105] Herein, α-glucosidase inhibitory activity of several metal(II) complexes **138–168** (Fig. 3) bearing different phthalocyanine derivatives **L60–L74** (Table 7) was discussed. Although all of them possessed square planar geometry; however, the electronic properties of metal ions and ligands were found to play a significant role in the inhibitory activity.

Zinc(II) complexes. Anti-α-glucosidase activity of a series of zinc(II) complexes (**138–145**, Fig. 3) with various substituted phthalocyanines (**L60**, **L62–L67**, **L72**, Table 7, entries 1, 3–8, 13) has been recently reported.[105–114] Among them, complex **143** containing sodium 2-mercaptoethanesulfonate moiety (**L66**, Table 7, entry 7) with IC_{50} value of 1.93 μM showed the best inhibitory effect comparing with acarbose as the reference drug (IC_{50} = 22.80 μM).[110] It should be noted that complex **142** (IC_{50} = 111.63 μM, acarbose = 189.20 μM) which had sodium 3-mercaptoethanesulfonate moiety (**L65**),[110] depicted 198-fold lower activity than **143**, indicating the effect of the position of substituents. Complex **138** having oxy methyl furan group (**L60**, Table 7, entry 1) had the worst inhibitory activity (IC_{50} = 902.83 μM) comparing with acarbose (IC_{50} = 0.38 μM).[106] Moreover, complexes **139** (IC_{50} = 7.08 μM, acarbose = 63.03 μM),[107] **141** (IC_{50} = 22.21 μM, acarbose = 51.45 μM),[108] and **144** (IC_{50} = 2.44 μM, acarbose = 22.80 μM),[110] displayed good inhibitory activity. However, it indicated the efficacy of involved ligands in the order of **L62** > **L64** > **L72**. Also, complexes **140**[109] and **145**[111] showed weak activity with IC_{50} values of 18.81 μM (acarbose = 15.92 μM) and 130.68 μM (acarbose = 22.80 μM), respectively.

Copper(II) complexes. Different Cu(II) complexes (**146–151**, Fig. 3) of phthalocyanine derivatives (**L60**, **L61**, **L64**, **L68**, **L69**, and **L72**, Table 7, entries 1, 2, 5, 9, 10, and 13) have been evaluated for their α-glucosidase inhibitory activity and compared with acarbose as the reference drug.[105,106,108–110,112] In this respect, the best activity was related to the complex **148** (IC_{50} = 0.81 μM, acarbose = 22.80 μM) containing 3,4-dimethoxyphenethoxy moiety (**L72**, Table 7, entry 13)[110] and the complex **146** (IC_{50} = 911.20 μM, acarbose = 0.38 μM) possessing oxy

Table 6 α-Glucosidase inhibitory activity of tetravalent metal complexes bearing hydrazide, picolinic acid (PicAs), and Schiff base ligands

Entry	Compounds	Structure number	IC_{50} (μM)	Ref.
1	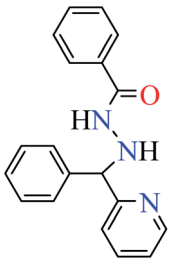	**L33**	Not reported	94[a]
	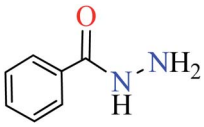	**L34**	Not reported	94[a]
	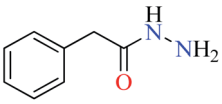	**L35**	NA	93[b]
	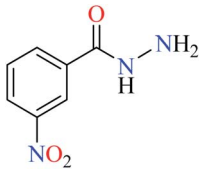	**L36**	NA	93[b]
	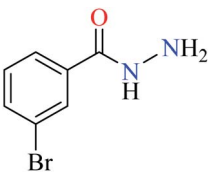	**L37**	NA	93[b]
	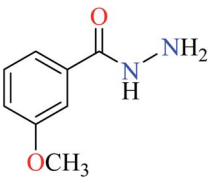	**L38**	NA	93[b]
	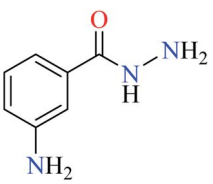	**L39**	NA	93[b]
	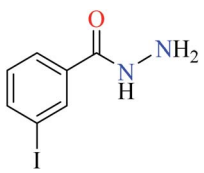	**L40**	NA	93[b]
	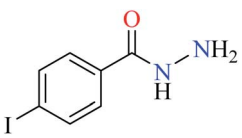	**L41**	NA	93[b]

Table 6 (*Contd.*)

Entry	Compounds	Structure number	IC_{50} (μM)	Ref.
	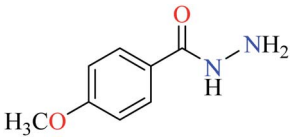	**L42**	NA	93[b]
	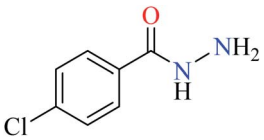	**L43**	NA	93[b]
	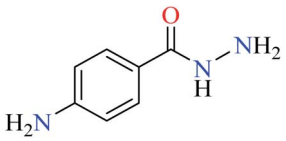	**L44**	NA	93[b]
	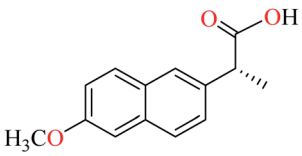	**L45**	Not reported	95[c]
	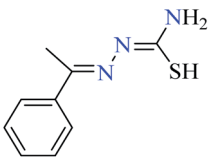	**L46**	Not reported	95[c]
	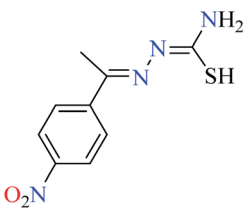	**L47**	Not reported	95[c]
	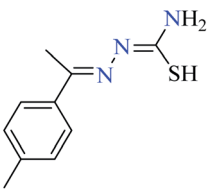	**L48**	Not reported	95[c]
	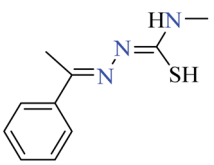	**L49**	Not reported	95[c]
	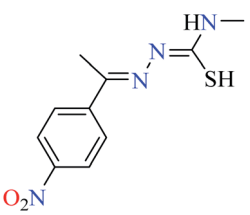	**L50**	Not reported	95[c]

Table 6 (*Contd.*)

Entry	Compounds	Structure number	IC_{50} (μM)	Ref.
	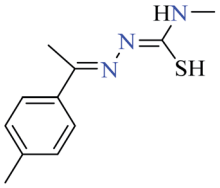	**L51**	Not reported	95[c]
	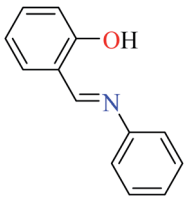	**L52**	Not reported	96[a]
	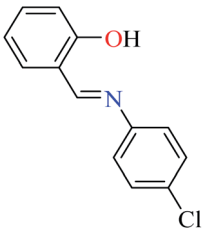	**L53**	Not reported	96[a]
	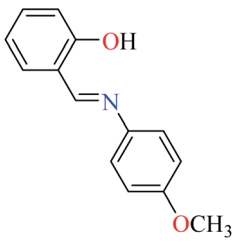	**L54**	Not reported	96[a]
	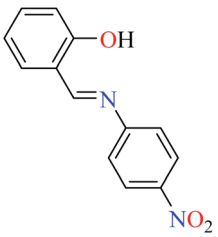	**L55**	22.72	96[a]
	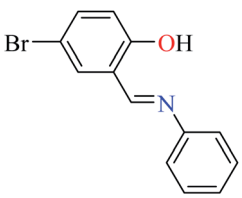	**L56**	Not reported	96[a]
	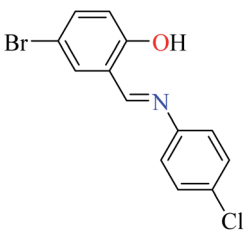	**L57**	Not reported	96[a]

Table 6 (*Contd.*)

Entry	Compounds	Structure number	IC_{50} (μM)	Ref.
	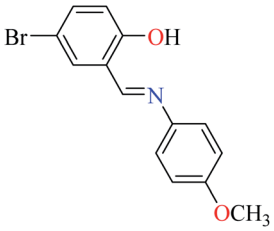	**L58**	74.11	96[a]
	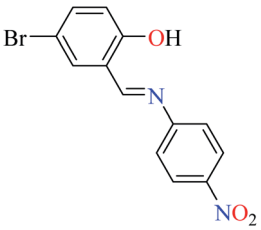	**L59**	245	96[a]
2	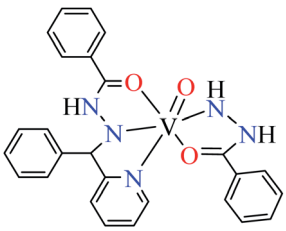			94[a]
	111 = [VO(**L33**)(**L34**)]	**111**	14.75	
3				93[b]
3a	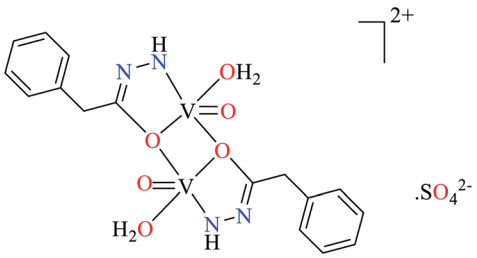			
	112 = $[(VO)_2(\mathbf{L35})_2(H_2O)_2]\cdot SO_4^{2-}$	**112**	10.70	
3b	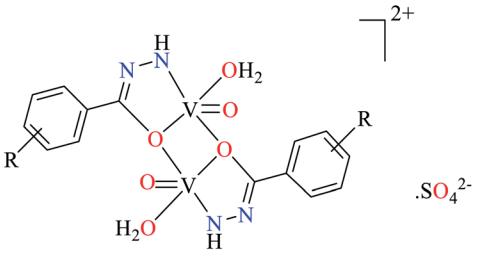			
	R = Br, OCH_3, I, NH_2, NO_2			
	113 = $[(VO)_2(\mathbf{L36})_2(H_2O)_2]$	**113**	67.00	
	114 = $[(VO)_2(\mathbf{L37})_2(H_2O)_2]$	**114**	20.10	
	115 = $[(VO)_2(\mathbf{L38})_2(H_2O)_2]$	**115**	0.68	
	116 = $[(VO)_2(\mathbf{L39})_2(H_2O)_2]$	**116**	12.50	
	117 = $[(VO)_2(\mathbf{L40})_2(H_2O)_2]$	**117**	800	
	118 = $[(VO)_2(\mathbf{L41})_2(H_2O)_2]$	**118**	758	
	119 = $[(VO)_2(\mathbf{L42})_2(H_2O)_2]$	**119**	38.00	
	120 = $[(VO)_2(\mathbf{L43})_2(H_2O)_2]$	**120**	13.50	
	121 = $[(VO)_2(\mathbf{L44})_2(H_2O)_2]$	**121**	16.40	

Table 6 (*Contd.*)

Entry	Compounds	Structure number	IC_{50} (μM)	Ref.
4	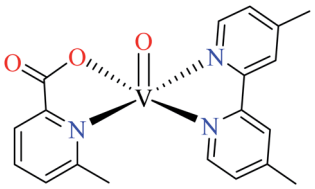			62[d]
	122 = [VO(**L11**)(**L12**)]	**122**	>600	
5	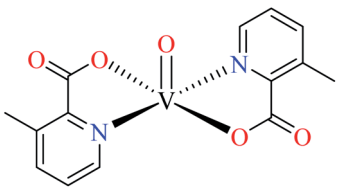			84[d]
	123 = [VO(**L17**)$_2$]	**123**	>600	
6	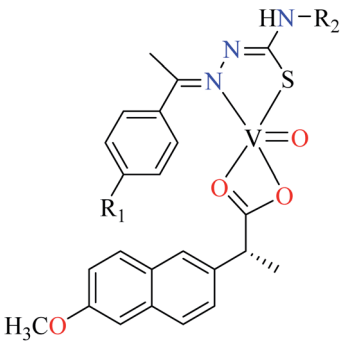			95[c]
	R_1 = H, NO_2, CH_3			
	R_2 = H, CH_3			
	124 = [VO(**L45**)(**L46**)]	**124**	Not reported clearly	
	125 = [VO(**L45**)(**L47**)]	**125**	Not reported clearly	
	126 = [VO(**L45**)(**L48**)]	**126**	Not reported clearly	
	127 = [VO(**L45**)(**L49**)]	**127**	Not reported clearly	
	128 = [VO(**L45**)(**L50**)]	**128**	Not reported clearly	
	129 = [VO(**L45**)(**L51**)]	**129**	Not reported clearly	
7	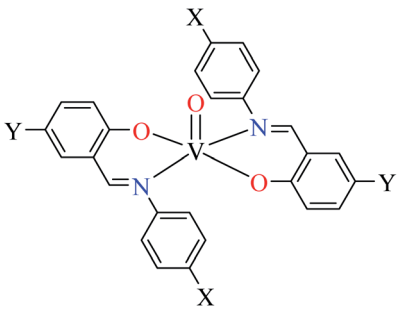			96[a]
	X = H, Cl, OCH_3, NO_2			
	Y = H, Br			
	130 = [VO(**L52**)$_2$]	**130**	2.11	
	131 = [VO(**L53**)$_2$]	**131**	13.12	
	132 = [VO(**L54**)$_2$]	**132**	1.26	
	133 = [VO(**L55**)$_2$]	**133**	1.26	
	134 = [VO(**L56**)$_2$]	**134**	16.92	
	135 = [VO(**L57**)$_2$]	**135**	Not reported	
	136 = [VO(**L58**)$_2$]	**136**	92.43	
	137 = [VO(**L59**)$_2$]	**137**	31.10	

[a] Acarbose as the reference drug (IC_{50} = 18.59 μM). [b] Acarbose as the reference drug (IC_{50} = 780 ± 0.28 μM). [c] Not reported. [d] Genistein as the reference drug (IC_{50} = 16.75 ± 0.23 μM).

Table 7 α-Glucosidase inhibitory activity of phthalocyanines

Entry	Compounds	Structure number	IC_{50} (μM)	Ref.
1	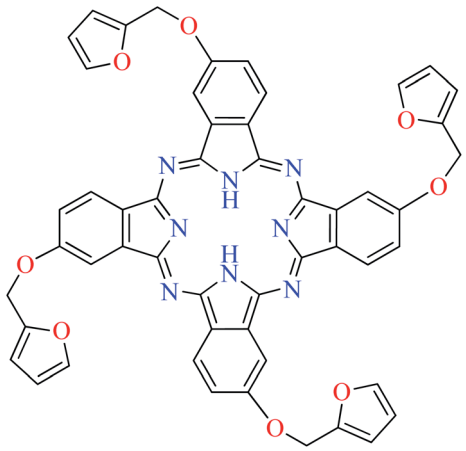	L60	1104.04	106[a]
2	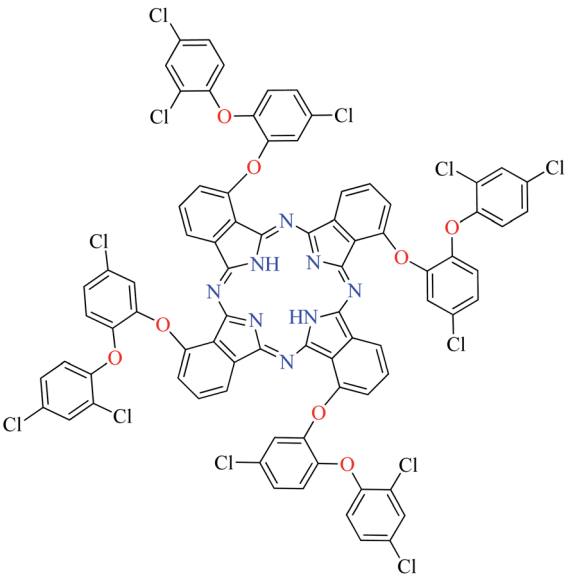	**L61**	158.66	105[b]
3	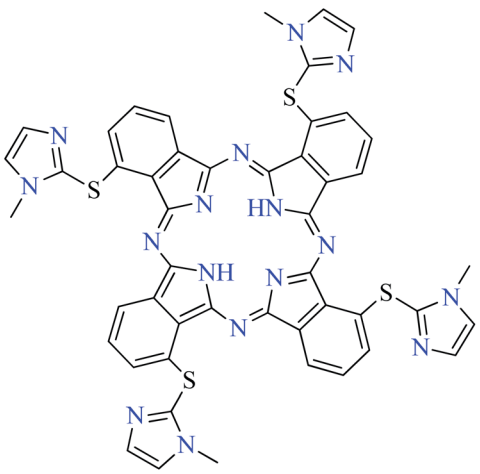	**L62**	Not reported	107[c]

Table 7 (*Contd.*)

Entry	Compounds	Structure number	IC_{50} (μM)	Ref.
4	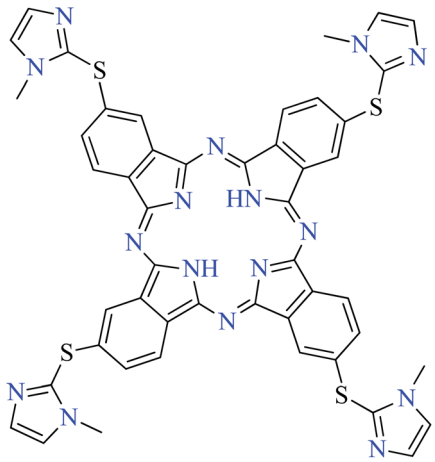	**L63**	Not reported	109[d]
5	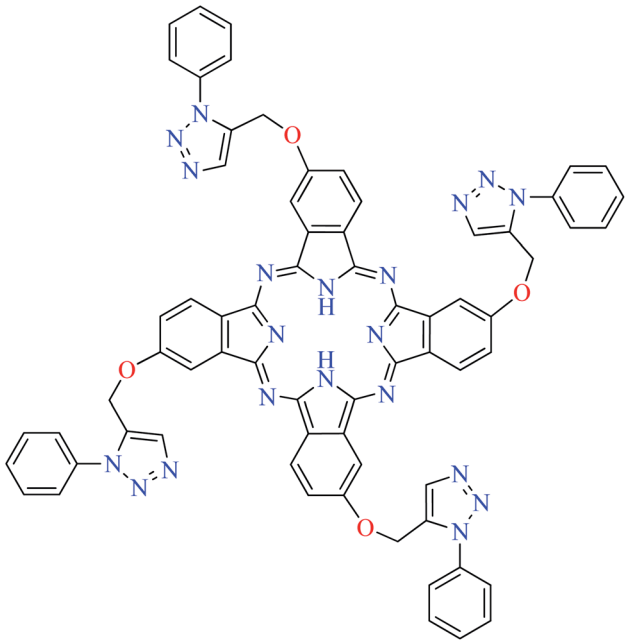	**L64**	11.65	108[e]
6	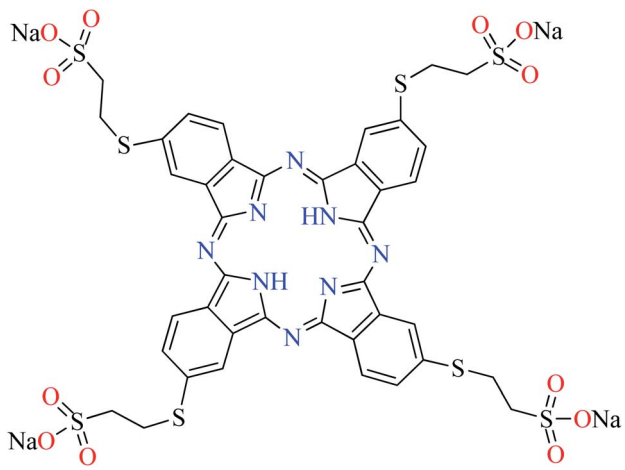	**L65**	Not reported	110[f]

Table 7 (*Contd.*)

Entry	Compounds	Structure number	IC_{50} (μM)	Ref.
7	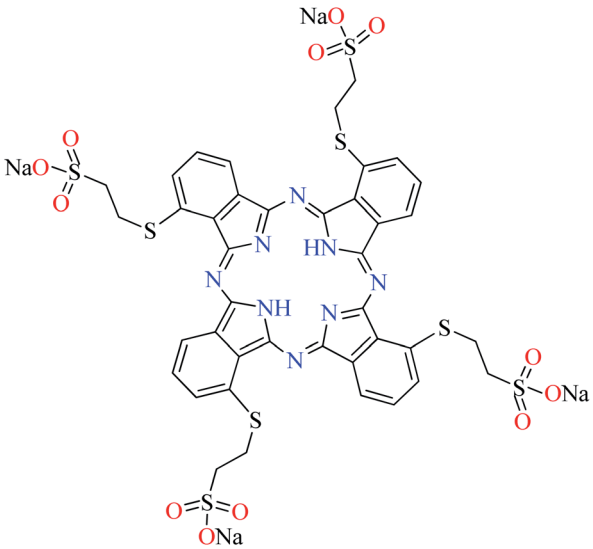	**L66**	Not reported	110[g]
8	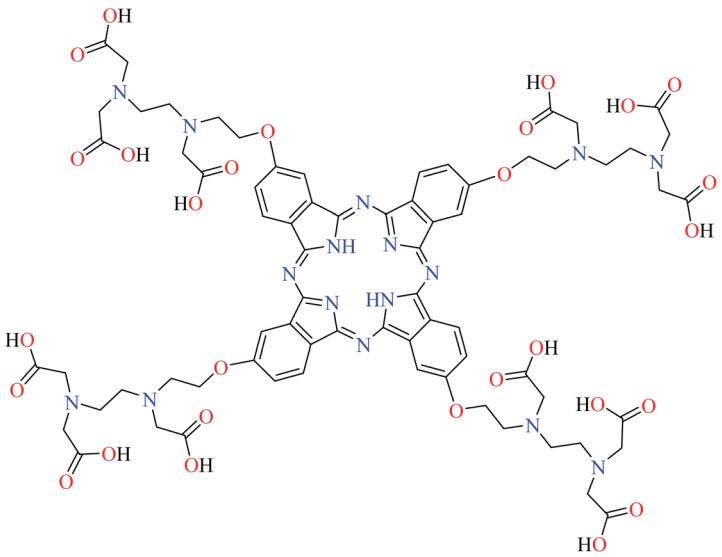	**L67**	Not reported	111[g]

Table 7 (*Contd.*)

Entry	Compounds	Structure number	IC_{50} (μM)	Ref.
9	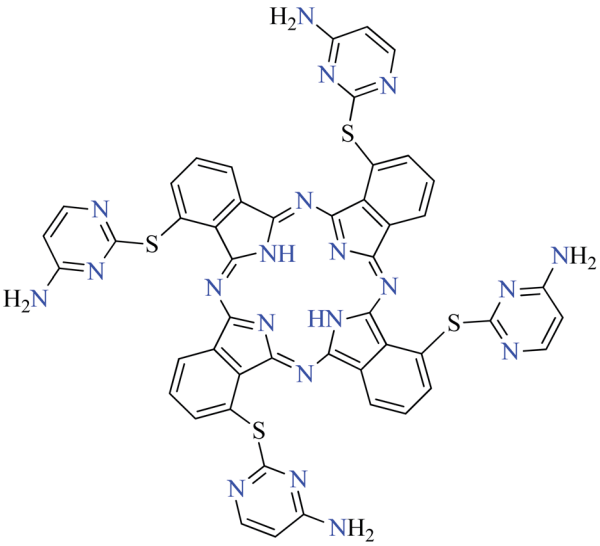	**L68**	Not reported	112[h]
10	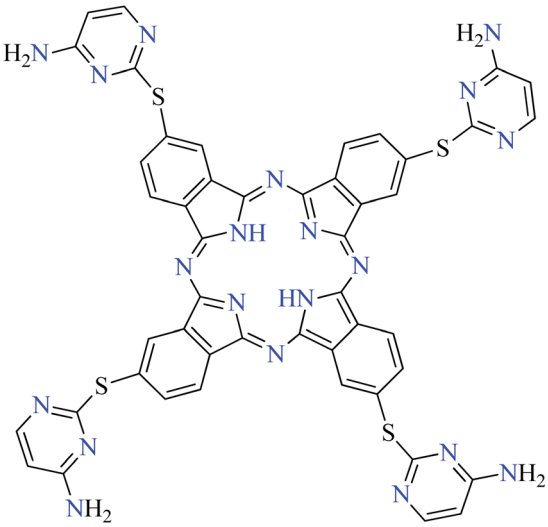	**L69**	Not reported	109[f]

Table 7 (*Contd.*)

Entry	Compounds	Structure number	IC_{50} (μM)	Ref.
11	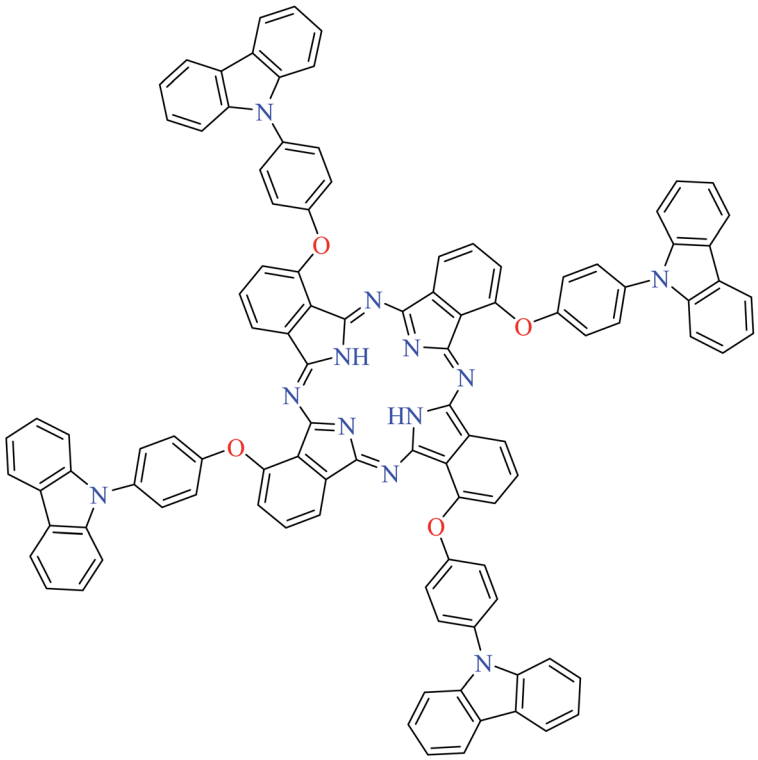	**L70**	Not reported	113[i]
12	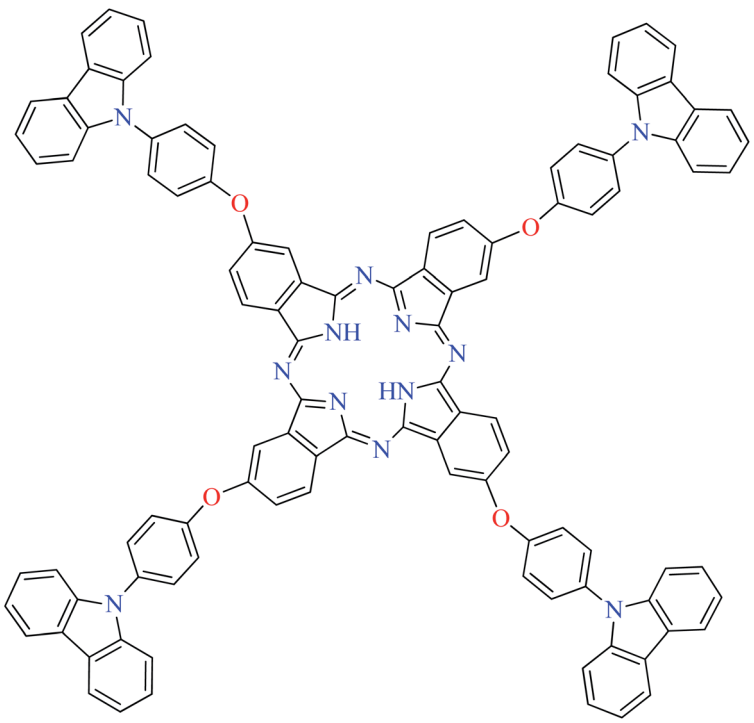	**L71**	Not reported	113[i]

Table 7 (*Contd.*)

Entry	Compounds	Structure number	IC_{50} (μM)	Ref.
13	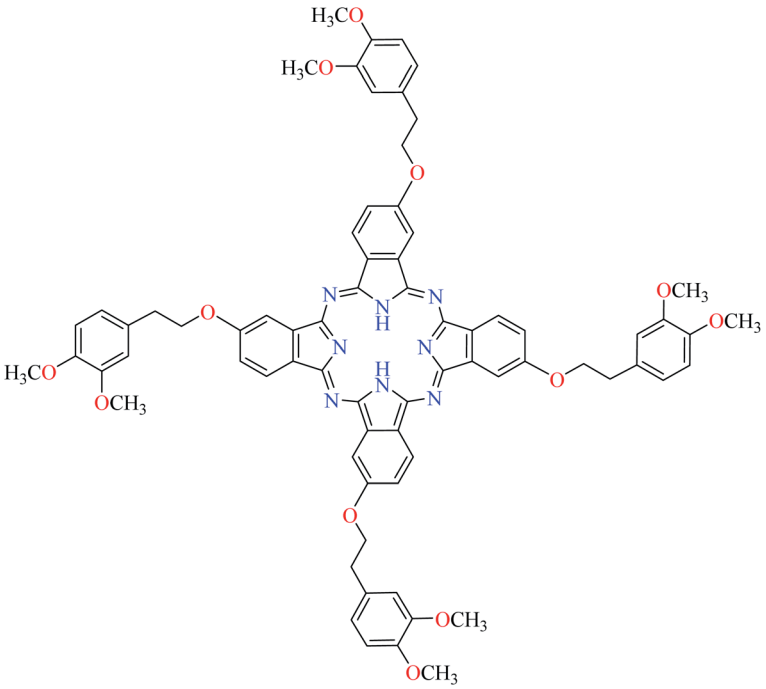	**L72**	Not reported	110[g]
14	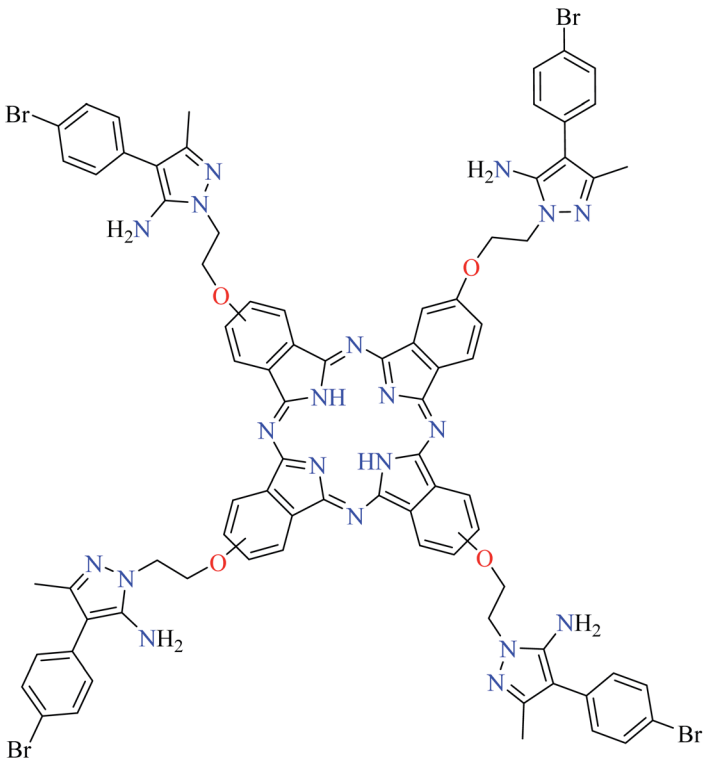	**L73**	Not reported	114[g]

Table 7 (*Contd.*)

Entry	Compounds	Structure number	IC_{50} (μM)	Ref.
15	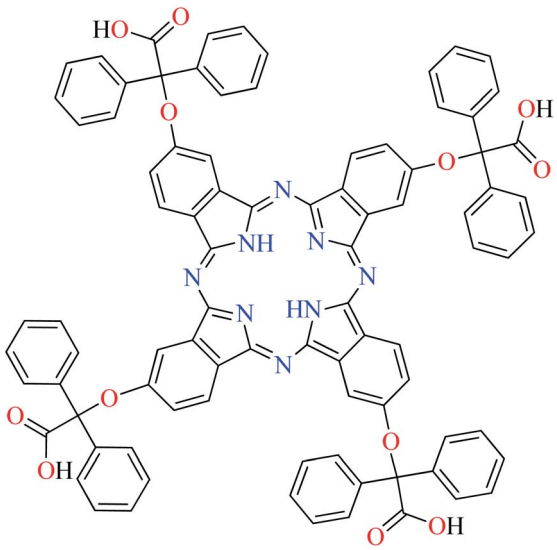	**L74**	Not reported	111[g]

[a] Acarbose as the reference drug (IC_{50} = 0.38 μM). [b] Acarbose as the reference drug (IC_{50} = 60.55 μM). [c] Acarbose as the reference drug (IC_{50} = 63.03 μM). [d] Acarbose as the reference drug (IC_{50} = 15.92 μM). [e] Acarbose as the reference drug (IC_{50} = 51.45 μM). [f] Acarbose as the reference drug (IC_{50} = 189.20 μM). [g] Acarbose as the reference drug (IC_{50} = 22.80 μM). [h] Acarbose as the reference drug (IC_{50} = 12.60 μM). [i] Acarbose as the reference drug (IC_{50} = 58.47 μM).

methyl furan group (**L60**, Table 7, entry 1) was the weakest inhibitor.[106] Moreover, α-glucosidase inhibitory effect of the copper(II) phthalocyanine **147** containing 1,2,3-triazole moiety (**L64**, Table 7, entry 5) was found to be relatively more active (IC_{50} = 42.14 μM) than acarbose (IC_{50} = 51.45 μM).[108] Complex **149** (IC_{50} = 25.12 μM) possessing 5-chloro-2-(2,4-dichlorophenoxy)phenol substituted phthalocyanine (**L61**, Table 7, entry 2) was also more potent than acarbose (IC_{50} = 60.55 μM).[105] Two Cu(II) phthalocyanine complexes **150**[112] and **151**[109] containing methylated amino thio pyrimidine moieties (**L68** and **L69**, Table 7, entries 9 and 10) depicted no significant inhibitory activity toward α-glucosidase as IC_{50} values were found as 10.08 μM (acarbose = 12.60 μM) and 104.52 μM (acarbose = 189.20 μM), respectively. It confirmed that the position of thio group connected to the aryl moiety is not very important.

Nickel(II) complexes. Evaluation of anti-α-glucosidase activity of a series of Ni(II) complexes (**152–154**, Fig. 3) coordinated with phthalocyanine derivatives (**L61**, **L64**, and **L73**, Table 7, entries 2, 5, and 14)[105,108,114] demonstrated that the substitutions on phthalocyanine moiety affected the inhibitory activity. Among those reported in the literature, complex **154** having 5-amino-4-aryl-3-methyl-1-oxylethyl pyrazole group (**L73**, Table 7, entry 14)[114] was the most potent compound (IC_{50} = 0.007 μM) comparing with acarbose (IC_{50} = 22.80 μM). However, complex **152** (IC_{50} = 26.18 μM, acarbose = 51.45 μM) having 1,2,3-triazole ligand (**L64**, Table 7, entry 5)[108] was found to be more potent than complex **153** having 5-chloro-2-(2,4-dichlorophenoxy)phenol group (**L61**, Table 7, entry 2)[105] (IC_{50} = 75.35 μM, acarbose = 60.55 μM). It showed that the presence of 5-membered nitrogen heterocycle connected to the phthalocyanine moiety is important for inducing desired inhibitory activity.

Cobalt(II) complexes. Co(II) phthalocyanines (**155–163**, Fig. 3) have shown good to weak α-glucosidase inhibitory activity based on different phthalocyanine derivatives (**L64**, **L67–L74**, Table 7, entries 5 and 8–15).[108–114] Considering the results revealed that Co(II) complex **162** (IC_{50} = 0.006 μM, acarbose = 22.80 μM) having 5-amino-4-aryl-3-methyl-1-oxylethyl pyrazole group (**L73**, Table 7, entry 14)[114] had the best inhibitory activity. Complexes **160** (**L70**, Table 7, entry 11)[113] and **161** (**L71**, Table 7, entry 12)[113] containing carbazole-phenoxy were also studied and the corresponding IC_{50} values were calculated as 26.57 and 3.05 μM, respectively comparing with acarbose (IC_{50} = 58.47 μM). It showed that the position of connection of phenoxy carbazole moiety to the phthalocyanines ring is important as complexes **161** having the substituent at 3-position was more potent than complexe **160** having the same group at 4-position. It should be noted that complex **157** (IC_{50} = 106.21 μM, acarbose = 22.80 μM) having (ethylenediamine-*N*,*N*′,*N*′-triacetic acid-*N*-2-ethyl)-oxy as the ligand (**L67**, Table 7, entry 8), showed no potent activity.[111]

Manganese(II) complexes. α-Glucosidase inhibitory activity of a series of Mn(II) complexes (**164–168**, Fig. 3) bearing phthalocyanine derivatives (**L60**, **L64**, **L70**, **L71**, and **L73**, Table 7, entries 1, 5, 11, 12, and 14) has been reported in the literature

and the IC_{50} values were obtained in the range of 0.002–695.37 μM comparing with acarbose as the standard drug.[106,108,113,114] Complex **168** containing 5-amino-4-aryl-3-methyl-1-oxylethyl pyrazole group (**L73**, Table 7, entry 14)[114] showed the most potent activity (IC_{50} = 0.002 μM, acarbose = 22.80 μM), while complex **164** having oxy methyl furan moiety (**L60**, Table 7, entry 1)[106] was the weakest inhibitor (IC_{50} = 695.37 μM, acarbose = 0.38 μM) among those Mn(II) phthalocyanines. Complexes **165** (IC_{50} = 30.01 μM, acarbose = 51.54 μM) having phenyl 1,2,3-triazole ligand (**L64**, Table 7, entry 5)[108] as well as **166** (IC_{50} = 25.93 μM, acarbose = 58.47 μM) (**L70**, Table 7, entry 11)[113] and **167** (IC_{50} = 15.82 μM, acarbose = 58.47 μM) (**L71**, Table 7, entry 12)[113] bearing carbazole-phenoxy group showed no significant difference in the inhibitory activity. However, as observed for the cobalt compartments, complex **167** with carbazole-phenoxy moiety at 3-position was found to be more potent than complex **166** with the same group at 4-position. The study of complex **165** with phenyl-1,2,3-triazole ring showed that the ligand was not very important in inducing α-glucosidase inhibitory activity comparing with 5-amino-4-aryl-3-methyl-1-oxylethyl pyrazole and carbazole-phenoxy derivatives.

Prospects and challenges

Evaluation of α-glucosidase inhibitory activity of metal complexes has recently absorbed the attention of researchers working on the field of treatment of T2DM. In this paper, the inhibitory activity of the first-row transition complexes toward α-glucosidase was reviewed.

α-Glucosidase inhibitory activity of divalent transition metal complexes 1–101(Tables 1–4)

Discussed metal centers coordinated to hydrazide, picolinic acid, Schiff base, and diamine moieties. Among them, Cu(II) complexes were usually found to be significant inhibitors, however, the complex of hydrazide moiety attracted more attention.

In the case of divalent transition metal complexes bearing hydrazide ligands **1–36** (Table 1):

• Complex **13** bearing **L5** was the most potent compound.

• Complexes of **L1**: complex **30** Mn(**L1**) showed the best inhibitory activity (IC_{50} = 45.63 μM) and replacement of Zn(II) afforded more than 2-fold reduction in the activity (IC_{50} = 101.29 μM). Cu(II) and Co(II) complexes of the same ligand were not active toward α-glucosidase.

• Complexes of **L2**: complex **10** Cu(**L2**) depicted the best anti-α-glucosidase activity (IC_{50} = 17.73 μM) and replacement of metal ion by Zn(II), Co(II), and Mn(II) afforded lower activity (IC_{50}s = 101.29, 66.48, and 143.21 μM, respectively).

• Complexes of **L3**: complex **11** Cu(**L3**) with IC_{50} value of 1.15 μM was found to the most active. Replacement of the metal ion by Zn(II) gave the lower activity (IC_{50} = 27.71 μM) and the order of activity in Co(II) and Mn(II) complexes followed a declining trend (IC_{50}s = 153.23 and 354.62 μM, respectively).

• Complexes of **L4**: complex **12** Cu(**L4**) was the most potent anti-α-glucosidase compound (IC_{50} = 18.91 μM). Complexes **4** Zn(**L4**) and **25** Co(**L4**) showed similar activity (IC_{50}s = 97.26 and 96.95 μM, respectively), however, lower than **12** Cu(**L4**). **33** Mn(**L4**) was completely inactive toward α-glucosidase.

• Complexes of **L5**: complex **13** Cu(**L5**) was the most potent inhibitor (IC_{50} = 0.15 μM) and the other M**L5** complexes were inactive toward α-glucosidase (Table 1, entry 2).

• Complexes of **L6**: complex **14** Cu(**L6**) was the most potent inhibitor (IC_{50} = 0.21 μM) and **6** Zn(**L6**) and **27** Co(**L6**) showed at least a 500 and 1000-fold reduction of activity with IC_{50} values of 121.19 and 213.30 μM, respectively.

• Complexes of **L7**: most complexes were inactive, only **35** Mn(**L7**) showed moderate activity (IC_{50} = 457.28 μM).

• Complexes of **L8**: **16** Cu(**L8**) represented the higher inhibitory effect (IC_{50} = 140 μM) than **7** Zn(**L8**) and **19** Ni(**L8**) with IC_{50} values of 180 and 200 μM, respectively.

• Complexes of **L9**: with the replacement of **L9**, no noteworthy change in the inhibitory activity of Cu(II), Zn(II), and Ni(II) complexes was observed. However, **17** Cu(**L9**) showed the best inhibition (IC_{50} = 170 μM). In fact, the presence of the hydroxyl group in **L9** did not have a significant effect on the inhibitory activity of the complexes.

• The inhibitory activity of **L10** as well as related Cu(II), Ni(II), Co(II), and Mn(II) complexes were not reported clearly (Table 1, entry 4).

In the case of divalent transition metal complexes bearing PicA ligands **37–64** (Table 2).

• Among the complexes **37–64**, complex **47** including Cu(II) metal center had the best inhibitory effect (IC_{50} = 2.91 μM) which was 5.7-fold more potent than genistein (IC_{50} = 16.57 μM), as the reference compound.

• Interestingly, three complexes **38**, **37**, and **35** with same ion center (Cu(II)) and structure showed different inhibitory effects. They differed only in one of the substituents.

• The order of inhibitory effect for **42–44**, complexes based on **L11** having water, pyridine, and thiocyanate ligands, respectively, with trigonal bipyramidal geometry was **42** (IC_{50} = 2.95 μM) > **43** (IC_{50} = 3.49 μM) > **44** (IC_{50} = 8.02 μM). It is apparent that the replacement of thiocyanate moiety in **44** and pyridine in **43** with the water ligand in **42** reduced the inhibition of α-glucosidase by approximately 2.71 and 1.18-fold, respectively. The difference for complexes **42** and **43** can be associated with the effect of the π-conjugation of the pyridine ligand. In addition, H-bonding interactions in **42** including a water ligand could increase the inhibitory activity.

• Furthermore, by replacing Zn(II) metal with Cu(II) in complex **42**, the inhibitory properties of **37** (IC_{50} = 546.04 μM) reduced almost 185-fold (Table 2, entry 2a). These results suggested that metal ions can play a significant role in enzyme inhibition due to their electronic properties. It seems that Cu(II) with d^9 electronic configuration is able to be more stable *via* changing its coordination geometry leading to the better interactions with enzyme. In the case of Zn(II) complexes in which the metal center possesses d^{10} electronic configuration, no structural changes are observed due to lacking crystal field stabilization energy (CFSE).

• All complexes which have the distorted octahedral geometry coordination (**38–41**, **48**, **49**, **51–55**, and **57–64**) were found to be weak inhibitors (IC_{50} > 440 μM), except Fe(II) complex **59** depicting moderate activity (IC_{50} = 97.33 μM). It can be drawn

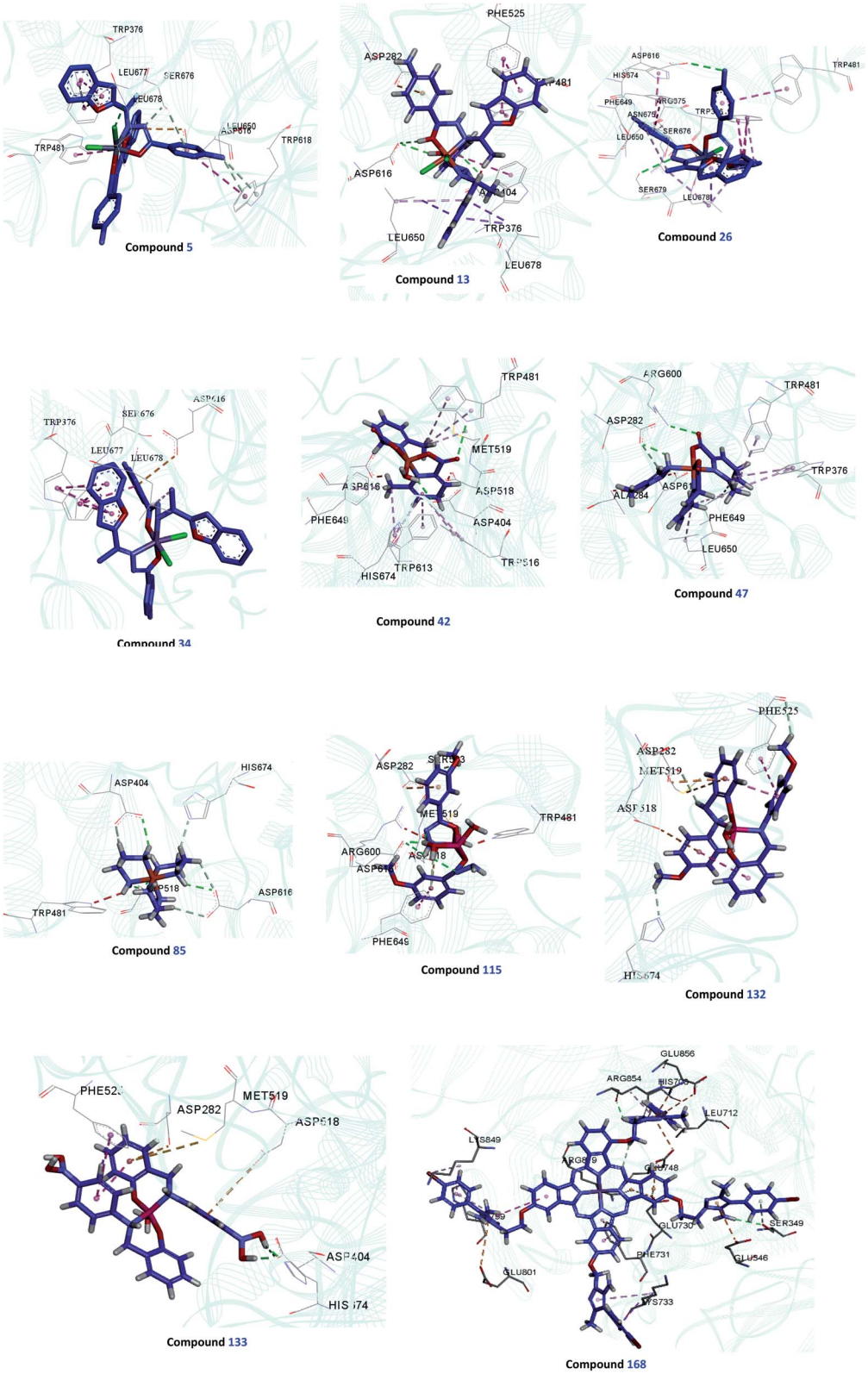

Fig. 4 Binding conformations of top rank docked compounds inside the active site of α-glucosidase.

from the obtained results that the presence of metal ion and the coordination environment of complexes can play a significant role in the inhibitory activity of the complex.

• There are two molecules of water in complexes **48**, **49**, **53**, **61**, and **62** (Table 2) which are expected to increase the number of H-bonding interactions and improve the inhibitory activity of

Table 8 Docking energy, biological IC_{50}, and interactions of compounds against α-glucosidase

Complex	Molegro score	IC_{50} (μM)	Residues	Interaction type
5	−90.0604	Not active	Trp616	Pi–donor hydrogen bond
			Ser676	Pi–donor hydrogen bond
			Leu678	Hydrogen bond
			Trp618	Pi–pi stack
			Trp376	Pi–pi stack
			Trp376	Pi–pi stack
			Asp616	Pii–anion
			Leu677	Unfavorable bump
			Leu678	Unfavorable bump
			Leu650	Unfavorable bump
			Ser676	Unfavorable bump
13	−156.14	0.15	Trp376	Pi–pi T-shaped
			Phe525	Pi–pi stacked
			Phe525	Pi–pi stacked
			Trp481	Pi–pi stacked
			Leu650	Pi-alkyl
			Asp282	Pi–anion
			Leu650	Pi–sigma
			Leu678	Pi–sigma
			Leu678	Pi–sigma
			Asp404	Hydrogen bond
			Asp616	Hydrogen bond
			Asp649	Hydrogen bond
26	−109.165	NA	Trp481	Pi–pi T-shaped
			His674	Pi–pi stack
			Phe649	Pi–pi stack
			Trp376	Pi–pi stack
			Arg375	Pi-alkyl
			Leu650	Pi-alkyl
			Leu677	Pi-alkyl
			Asp616	Hydrogen bond
			Ser679	Hydrogen bond
			Leu678	Pi–sigma
			Asn675	Unfavorable bump
			Ser676	Unfavorable bump
			Leu677	Unfavorable bump
			Leu678	Unfavorable bump
34	−74.292	NA	Trp376	Pi–pi T-shaped
			Trp376	Pi–pi stack
			Trp376	Pi–pi stack
			Leu678	Pi-alkyl
			Asp616	Pi–anion
			Ser676	Unfavorable bump
			Leu677	Unfavorable bump
			Leu677	Unfavorable bump
42	−110.0231	2.95	Trp481	Pi-alkyl
			Trp516	Pi-alkyl
			Trp519	Pi-alkyl
			Trp613	Pi-alkyl
			Phe649	Pi-alkyl
			His674	Pi-alkyl
			Asp404	Hydrogen bond
			Trp481	Hydrogen bond
			Asp518	Unfavorable bump
			Asp616	Unfavorable bump
47	−136.527	2.91	Trp376	Pi-alkyl
			Trp376	Pi-alkyl
			Trp481	Pi-alkyl
			Phe649	Pi-alkyl

Table 8 (*Contd.*)

Complex	Molegro score	IC_{50} (μM)	Residues	Interaction type
			Phe649	Pi-alkyl
			Phe650	Pi-alkyl
			Asp282	van der Waals
			Asp616	van der Waals
			Asp282	Hydrogen bond
			Met519	Hydrogen bond
			Ala284	Unfavorable bump
			Asp616	Unfavorable bump
85	−133.7351	0.47	Asp404	van der Waals
			Asp404	van der Waals
			Asp616	van der Waals
			Asp616	van der Waals
			His674	van der Waals
			Asp404	Hydrogen bond
			Asp518	Hydrogen bond
			Asp518	Hydrogen bond
			Asp518	Hydrogen bond
			Trp481	Unfavorable bump
115	−129.3691	0.68	Ser523	Carbon hydrogen bond
			Ser523	Carbon hydrogen bond
			Phe649	Pi–pi stack
			Asp282	Pi–anion
			Asp518	Hydrogen bond
			Asp616	Hydrogen bond
			Asp616	Hydrogen bond
			Trp481	Unfavorable bump
			Met519	Unfavorable bump
			Arg600	Unfavorable bump
132	−126.219	1.26	Phe525	Pi–pi T-shaped
			Asp282	Pi–anion
			Asp518	Pi–anion
			Met519	Pi–sulfur
			Asp282	Carbon hydrogen bond
			Phe525	Carbon hydrogen bond
			His674	Carbon hydrogen bond
133	−139.723	1.26	Phe525	Pi–pi T-shaped
			Asp282	Pi–anion
			Asp518	Pi–anion
			Met519	Pi–sulfur
			Phe525	Pi–sigma
			Asp404	Hydrogen bond
			Asp404	Hydrogen bond
			His674	Hydrogen bond
168	−237.455		Glu346	Pi–anion
			Ser349	H-bond
			Ser349	H-bond
			His708	H-bond
			Leu712	Alkyl
			Glu730	Pi–anion
			Glu730	Pi–anion
			Phe731	Pi–pi T shaped
			Phe731	Pi–pi T shaped
			Lys733	Pi-alkyl
			Lys733	Pi–sigma
			Glu748	Pi–anion
			Glu748	Pi–anion
			His799	Pi–pi T shaped
			His799	Pi-alkyl
			Glu801	Pi–anion
			Arg819	Pi–cation

Table 8 (*Contd.*)

Complex	Molegro score	IC_{50} (μM)	Residues	Interaction type
			Lys849	Alkyl
			Lys849	Pi-alkyl
			Arg854	H-bound
			Arg854	Pi-alkyl
			Arg854	Pi–cation
			Glu856	Pi–anion

the complexes. However, this was not observed and the same IC_{50} values were obtained as reported for other distorted octahedral tris chelates complexes.

• According to Table 2, entry 4c, complexes **59** and **60**, including Fe(II) metal ion, with the same coordination geometry showed different inhibitory effects. It should be noted that complex **59** (IC_{50} = 97.33 μM) having a methyl substitution group at 6-position, displayed almost 7.5-fold increase in the activity comparing with **60** (IC_{50} = 724.25 μM) which has the same substituent at 3-position of the pyridine ring. Therefore, it can be concluded that in addition to the change of the central metal, the presence of a substituent at different positions can change the α-glucosidase inhibitory effect of a complex.

• Zn(II) **38** and Ni(II) **50** complexes (Table 2, entry 5) containing **L11** and **L12** (Table 2, entry 1) mixed ligands and two methyl groups at 4-position of 2,2′-bipyridyl ligand (**L12**), showed no inhibitory activity (IC_{50} = >600 μM). They were similar to **59** from structure point of view.

• Comparing the inhibitory activity of complexes **39**, **46**, and **55** (Table 2, entry 6) having **L11** and **L13** mixed-ligand revealed that there is no a significant difference between IC_{50} values of these complexes. Zn(II) and Co(II) complexes with a distorted octahedral geometry showed weak activity (IC_{50} > 600 μM) and Cu(II) complex that had a distorted trigonal bipyramidal geometry revealed better anti-α-glucosidase activity (IC_{50} = 513.10 μM). It should be noted that the synthesized ligands were not active toward α-glucosidase.

• The IC_{50} values of the synthesized complexes of Zn(II), Cu(II), Ni(II), Mn(II), and Co(II) metals with mixed-ligands including **L11** and **L14** showed that except Cu(II) complex **47** (IC_{50} = 2.91 μM), the variation of metals in coordination did not affect the inhibition of α-glucosidase enzyme (Table 2, entry 7). The IC_{50} value of Cu(II) complex was approximately 6-fold higher than genistein as the reference drug (IC_{50} = 16.575 μM). Also, it was >206-fold more potent than other complexes (IC_{50} > 600 μM).

• The activity of complexes **52**, **57**, **58**, and **64** (IC_{50} > 600 μM) bearing **L11** and **L18** showed that distorted octahedral geometry had no effect on the inhibition of α-glucosidase.

• Among metal(II) complexes having PicA derivatives (**37–64**), only Cu(II) complexes **42** (IC_{50} = 2.95 μM) and **47** (IC_{50} = 2.91 μM) depicted strong inhibitory properties.

• Comparison of the inhibitory activity of Cu(II) coordinated to **L11** with same geometry of distorted trigonal bipyramidal (**42–47**) demonstrated that those having two **L11** ligands (**42–44** and **47**, $IC_{50} \leq 8$ μM) were much more potent than complexes containing one **L11** ligand (**45** and **46**, IC_{50} > 500 μM).

In the case of divalent transition metal complexes bearing Schiff base ligands **65–68** (Table 3):

• These complexes have not been widely investigated and only Zn(II) complexes were reported. Complex **68** bearing naphthalene moiety depicted the highest activity toward α-glucosidase both yeast and rat intestinal enzymes.

In the case divalent transition metal complexes bearing diamine ligands **69–101** (Table 4):

• Diamine complexes with the central metal Zn(II), Cu(II), Ni(II), and Co(II) having distorted octahedral structures did not demonstrate significant inhibitory potency. Among these complexes, only Cu(II) complex **85** possessing **L28** ligand revealed better IC_{50} value (IC_{50} = 0.47 mg mL^{-1}) than other metal compounds.

α-Glucosidase inhibitory activity of trivalent transition metal complexes 102–110 (Table 5)

A limited number of studies have investigated the α-glucosidase inhibitory activity of trivalent metal transition complexes in comparison to divalent complexes.

• Cr(III) complexes were generally found to be more potent than those Fe(III). The best inhibitory effect was shown by complex **107** with an IC_{50} value of 28.7 μM, which is approximately 14.5-fold higher than acarbose (IC_{50} = 418.0 μM), used as a reference compound.

• The hydroxamic acid ligand induced more important activity than PicA ligand. However, the electronic property of substituents on the hydroxamic acid moiety was significant. Complex **107** lacking substituents was more potent than **108** (IC_{50} = 69.28 μM), **109** (IC_{50} = 355.90 μM) and **110** (IC_{50} = 169.50 μM), possessing CH_3, OCH_3, and Cl, respectively. It seemed that electron-donating *via* a strong electron donating group (OMe) or inductive effect (Cl) deteriorated inhibitory activity.

• In one case, the complex of PicA ligand (**106**) showed relatively good activity which found to be more active than **109** and **110**. It seems that the presence of water as the ligand had a supportive role. Replacement of water by other ligands reduced or deleted the inhibitory activity.

α-Glucosidase inhibitory activity of tetravalent transition metal complexes 111–137 (Table 6)

• Complex **115** (IC_{50} = 0.68 μM) having **L38** with *meta*-methoxy substitution showed the most potent inhibitory activity. While

complex **119** (IC_{50} = 38 μM) bearing **L42** in which OCH_3 group was at *para* position displayed a reduction by approximately 56-fold in the inhibitory activity.

• Among hydrazide vanadyl complexes (**111–121**), the lowest inhibitory activity belonged to the complexes **117** (IC_{50} = 800 μM) and **118** (IC_{50} = 758 μM) containing **L36** and **L37** ligands with iodine substitution at *meta* and *para* positions, respectively. This may be related to the steric hindrance of iodine substituent.

• PicA vanadyl complexes (**122** and **123**) with distorted square pyramidal geometry showed no activity against α-glucosidase.

• Among Schiff base vanadyl complexes (**124–137**) possessing square pyramidal geometry, **132** and **133** including **L54** and **L55**, having strong electron-donating (OMe) and electron-withdrawing (NO_2) groups, respectively, showed the best inhibitory effect (IC_{50} = 1.26 μM).

α-Glucosidase inhibitory activity of phthalocyanine transition metal complexes 138–168 (Table 7)

• Considering the most potent complexes of the first row transition metals with phthalocyanines revealed that the best inhibitory activity was related to the complexes **168**, **162**, and **154** possessing 5-amino-4-aryl-3-methyl-1-oxylethyl pyrazole substituted phthalocyanine (**L73**, Table 7, entry 14). It should be noted that the inhibitory activity of complex **168** (IC_{50} = 0.002 μM, acarbose = 22.80 μM) was much more significant than other phthalocyanine complexes (**138–168**, Fig. 3).

• Complexes **138**, **146**, and **164** possessing oxy methyl furan group (**L60**, Table 7, entry 1) demonstrated the lowest inhibitory activity.

• No comparable inhibitory activity was found between **L64**-based (phenyl-1,2,3-triazole substituted phthalocyanine) complexes **141**, **147**, **152**, **155** and **165** of Zn(II), Cu(II), Ni(II), Co(II), and Mn(II), respectively.

• The inhibitory activity of metallo(Zn(II), Cu(II), and Co(II)) phthalocyanine complexes (**144**, **148**, and **156**) having **L72** (3,4-dimethoxyphenethoxy substituted phthalocyanine) was approximately 9-fold, 28-fold, and 25-fold more potent than acarbose, respectively.

• Among the copper(II) (**149**) and nickel(II) (**153**) complexes containing **L61** 5-chloro-2-(2,4-dichlorophenoxy)phenol substituted phthalocyanine, **149** showed relatively good activity, which was more potent than **153**. It confirms that changing the metal ion affect the inhibitory activity of the complexes.

• Complexes of Cu(II) and Co(II), **151** and **159**, having **L69** (methylated amino thio pyrimidine substituted phthalocyanine) showed no noteworthy changes for the anti-α-glucosidase activity. However, **159** Co(**L69**) exhibited approximately 2-fold higher activity than acarbose.

• Among complexes **160** Co(**L70**) and **161** Co(**L71**) as well as complexes **166** Mn(**L70**) and **167** Mn(**L71**), **161** showed very good inhibitory activity (IC_{50} = 3.05 μM), however, the others more potent than acarbose.

Conclusions and future perspectives

Survey of literature on novel α-glucosidase inhibitors led us to metal complexes, which have shown versatile properties from both structural and electronic points of view to induce desired activity. Hence, they have occupied a particular attention in the field of enzyme inhibition comparing with small organic molecules. Herein, we focused on the anti-α-glucosidase activity of complexes as a novel and efficient tool in the treatment of T2DM. The efficacy of metal complexes comes back to the fact that free ligands usually have not been active or had a low activity, whereas the corresponding complexes depicted high inhibitory activity. In this respect, the first-row transition metal complexes were in the center of attention. However, their exact mechanism of action toward enzyme is not definitely clear. In this respect, the interaction mode of some potent compounds **5**, **13**, **26**, **34**, **42**, **47**, **85**, **115**, **132**, **133**, and **168** were investigated (Fig. 4).

The inhibitory activity of discussed complexes in this review and probable mechanism of action can be explained from different perspectives of electronic and structural properties.

• The electronic property of the metal complexes plays a significant role in the anti-α-glucosidase activity. The electronic property is depended on the oxidation state of central metal ions and monodentate ligands, which have been coordinated to the central metal. According to the study of Gu *et al.*,[115] metal ions can be considered as the versatile candidates for the inhibition of α-glucosidase. Various metal ions such as Cu^{2+}, Ni^{2+}, Mg^{2+}, Fe^{2+}, Fe^{3+}, Hg^{2+}, Zn^{2+}, Ca^{2+}, Pb^{2+}, Ag^{+}, V^{4+}, V^{5+}, Al^{3+}, B^{3+}, and Mn^{2+} were evaluated for their *in vitro* α-glucosidase inhibitory activity.

(i) Transitions state metals such as copper, vanadium, nickel, and zinc were found to be much more active that main group metals.

(ii) Among divalent cations, Cu^{2+} was the most potent ion (IC_{50} = 2.28 μM). However, it depicted the highest activity in the studied series of ions. Trivalent cations were not found to be important inhibitors as Fe^{3+} and Al^{3+} were completely inactive and B^{3+} could weakly inhibit α-glucosidase (IC_{50} = 2291 μM). In the case of tetravalent and higher metal ions (V^{4+} and V^{5+}), good activity was observed. V^{4+} also showed much more inhibition potency (IC_{50} = 44.8 μM) than that of V^{5+}. Our survey on the inhibitory activity of the first-row transition metal complexes confirmed the high efficacy of Cu^{2+} complexes among divalent complexes. Trivalent complexes were also low active and V^{4+} complexes possessed moderate to good potency in the series of tetravalent and higher complexes. It seems that the role of electronic property of metal complexes is important in α-glucosidase inhibition and also is in good agreement with those of free metal ions property.[115]

• The structural property of the metal complexes is also an important factor, which should be taken in account for anti-α-glucosidase activity.

(i) The literature review indicated that the α-glucosidase inhibitory activity of metal(II) complexes was completely depended on geometry of the complex. For example, in the

series of M(II) complexes **40**, **47**, **51**, **56**, and **63** reported by Avcı *et al.* complex **47** with TBP geometry showed the best inhibitory activity (IC_{50} = 2.91 μM) when compared with other complexes possessing octahedral geometry (**40**, **51**, **56**, and **63**) (IC_{50} > 600 μM).[63]

(ii) The spatial hindrance of the ligand, the presence of electron-donating or electron-withdrawing substituents as well as their position on the ligand moiety were crucial factors which affected the structural property of the metal complexes. For instance, two Fe(II) complexes **59** and **60** having 3- and 6-methylpicolinic acid (**L11** and **L17**), respectively, with the same geometry revealed different inhibitory activity. Changing the position of methyl group from 6- of **PicA** moiety in complex **60** (IC_{50} = 724.25 μM) to 3- in complex **59** (IC_{50} = 97.33 μM) led to a 7-fold increase of activity.[67]

• The mechanism of α-glucosidase inhibitory activity of the first row transition metal complexes can be investigated from different aspects.

(i) According to Gu *et al.* report,[115] metal ions are enable to inhibit the enzyme through impact on the secondary structure of the enzyme by reduction of α-helix to β-sheet ratio which is occurred by weakening the hydrophobic property.

(ii) Molecular docking of some complexes (**5**, **13**, **26**, **34**, **42**, **47**, **85**, **115**, **132**, and **133**, and **168**) were performed to predict binding conformations and interactions between ligands and the binding site of α-glucosidase.

As far as we know no study was performed to fully evaluate and compare different software to apply in docking of organometallic complexes. All of the complexes were drawn using GaussView 6.0 and were converted to the energetically most stable structure using energy minimization with Hyperchem and Gaussian program. The ligands and protein were converted to their proper readable file format based on the software applied. Different molecular docking programs were applied, to detect similar trends between biological results and *in silico* outputs. In this context, different docking software named Autodock tools (version 4.2), Gold (Hermes v1.3.1), IGEM (version, 2.1) and Molegro Virtual Docker dock (version, 6.0) software was conducted. Also, various fitness functions, scoring functions, and algorithms were applied. According to Table 8, Molegro Virtual Docker dock software demonstrated more power to properly predict the bio-results in comparison with the rest of the docking programs used in this study. Molegro Virtual Docker software with Max iterations 1500, population size 200, energy threshold 100, and the number of run 100 with MolDock scoring function recorded the best results. The final visualization of the docked structure was performed using Discovery Studio Visualizer 2.5 (Accelrys Software Inc., San Diego, CA, USA). As can be seen, the potent complex was **13** with Molegro Score of −156.14 and IC_{50} value of 0.15 μM followed by **85** (Molegro Score = −133.73 and IC_{50} = 0.47 μM) and **115** (Molegro Score = −129.37 and IC_{50} = 0.68 μM). Our preliminary evaluations showed that the most active derivatives participated in the interactions with Asp404 and Asp282. Also, it was exhibited that binding energy below ≥−100 can be considered as not active while −110≥ categorized as potent inhibitors. The deviation to predict α-glucosidase inhibitory activity can be seen in compound **26**. The predicted binding pose of top-ranked docked complexes was presented in Fig. 4. All the residues involved in molecular interaction are shown in line form and colored by atom types in which carbon is depicted in grey and oxygen in red.

The main point is that complex **168** behaved differently against α-glucosidase. The enzyme kinetic study showed that it was a non-competitive inhibitor and it binds to the enzyme at a location other than the active site. As a result, the maestro sitemap tool was applied to find the possible cavity of the enzyme. Five possible binding sites were detected on the surface of the enzyme which can be suitable for non-competitive inhibition. Next, **168** as the potent inhibitor was docked on all of the potential binding sites of the enzyme. The cavity with Ser349 His708, Leu712, Glu730, Glu801, and Arg819 residue (reported in Table 8) was selected as an allosteric site. Considering the Moledock score results, **168** participated in several interactions with the allosteric binding site which justifies its potency.

Even with all the significant improvements in the computational study in drug discovery, proper prediction of how ligand binds to its target is an extremely challenging task. It is important to note that no specific docking software or scoring function exists, that can be successfully applied to all molecular docking studies, due to the variability in nature of the ligands and its type of inhibition. However, according to our preliminary study, Molegro Virtual Docker software had more power to properly predict binding energy of organic metallic compounds against α-glucosidase.

Author contributions

Marzieh Sohrabi and Mohammad Reza Binaeizadeh searched databases and prepared the original draft. Aida Iraji performed docking study. Bagher Larijani and Mohammad Mahdavi analysed the results. Mina Saeedi edited the manuscript and supervised all steps.

Conflicts of interest

There are no conflicts to declare.

Acknowledgements

The authors acknowledged partial support from Tehran University of Medical Sciences.

References

1 A. Bastaki, *Int. J. Diabetes Mellitus*, 2005, **13**, 111.
2 W. Sami, T. Ansari, N. S. Butt and M. R. Ab Hamid, *Int. J. Health Sci.*, 2017, **11**, 65.
3 Y.-G. Chen, P. Li, P. Li, R. Yan, X.-Q. Zhang, Y. Wang, X.-T. Zhang, W.-C. Ye and Q.-W. Zhang, *Molecules*, 2013, **18**, 4221–4232.
4 R. K. Campbell, *J. Am. Pharmaceut. Assoc.*, 2009, **49**, S3–S9.

5 G. A. Colditz, W. C. Willett, M. J. Stampfer, J. E. Manson, C. H. Hennekens, R. A. Arky and F. E. Speizer, *Am. J. Epidemiol.*, 1990, **132**, 501–513.
6 G. A. Colditz, W. C. Willett, A. Rotnitzky and J. E. Manson, *Ann. Intern. Med.*, 1995, **122**, 481–486.
7 S. P. Helmrich, D. R. Ragland, R. W. Leung and R. S. Paffenbarger Jr, *N. Engl. J. Med.*, 1991, **325**, 147–152.
8 F. B. Hu, R. J. Sigal, J. W. Rich-Edwards, G. A. Colditz, C. G. Solomon, W. C. Willett, F. E. Speizer and J. E. Manson, *JAMA*, 1999, **282**, 1433–1439.
9 J. E. Manson, U. A. Ajani, S. Liu, D. M. Nathan and C. H. Hennekens, *Am. J. Med.*, 2000, **109**, 538–542.
10 J. Salmeron, J. E. Manson, M. J. Stampfer, G. A. Colditz, A. L. Wing and W. C. Willett, *Jama*, 1997, **277**, 472–477.
11 M. J. Knol, J. W. Twisk, A. T. Beekman, R. J. Heine, F. J. Snoek and F. Pouwer, *Diabetologia*, 2006, **49**, 837–845.
12 C.-Y. Cai, L. Rao, Y. Rao, J.-X. Guo, Z.-Z. Xiao, J.-Y. Cao, Z.-S. Huang and B. Wang, *Eur. J. Med. Chem.*, 2017, **130**, 51–59.
13 J. Zhen, Y. Dai, T. Villani, D. Giurleo, J. E. Simon and Q. Wu, *Bioorg. Med. Chem.*, 2017, **25**, 5355–5364.
14 S. T. Assefa, E.-Y. Yang, S.-Y. Chae, M. Song, J. Lee, M.-C. Cho and S. Jang, *Plants*, 2020, **9**, 2.
15 H. B. B. Ag, *Eur. J. Clin. Invest.*, 1994, **24**, 3–10.
16 S. Chiba, *Biosci., Biotechnol., Biochem.*, 1997, **61**, 1233–1239.
17 M. Saeedi, A. Hadjiakhondi, S. Mohammad Nabavi and A. Manayi, *Curr. Top. Med. Chem.*, 2017, **17**, 428–440.
18 K. Papoutsis, J. Zhang, M. C. Bowyer, N. Brunton, E. R. Gibney and J. Lyng, *Food Chem.*, 2020, 128119.
19 S. Fattaheian-Dehkordi, R. Hojjatifard, M. Saeedi and M. Khanavi, *Evidence-Based Complementary Altern. Med.*, 2021, 2021.
20 D. Shareghi-Boroujeni, A. Iraji, S. Mojtabavi, M. A. Faramarzi, T. Akbarzadeh and M. Saeedi, *Bioorg. Chem.*, 2021, **111**, 104869.
21 M. Saeedi, M. Raeisi-Nafchi, S. Sobhani, S. S. Mirfazli, M. Zardkanlou, S. Mojtabavi, M. A. Faramarzi and T. Akbarzadeh, *Mol. Diversity*, 2020, 1–11.
22 M. Saeedi, M. Mohammadi-Khanaposhtani, M. S. Asgari, N. Eghbalnejad, S. Imanparast, M. A. Faramarzi, B. Larijani, M. Mahdavi and T. Akbarzadeh, *Bioorg. Med. Chem.*, 2019, **27**, 115148.
23 M. Saeedi, M. Mohammadi-Khanaposhtani, P. Pourrabia, N. Razzaghi, R. Ghadimi, S. Imanparast, M. A. Faramarzi, F. Bandarian, E. N. Esfahani and M. Safavi, *Bioorg. Chem.*, 2019, **83**, 161–169.
24 Z. Liu and S. Ma, *ChemMedChem*, 2017, **12**, 819–829.
25 K. Pedrood, M. Sherafati, M. Mohammadi-Khanaposhtani, M. S. Asgari, S. Hosseini, H. Rastegar, B. Larijani, M. Mahdavi, P. Taslimi and Y. Erden, *Int. J. Biol. Macromol.*, 2021, **170**, 1–12.
26 M. S. Asgari, M. Mohammadi-Khanaposhtani, Z. Sharafi, M. A. Faramarzi, H. Rastegar, E. N. Esfahani, F. Bandarian, P. R. Rashidi, R. Rahimi and M. Biglar, *Mol. Diversity*, 2021, **25**, 877–888.
27 M. Sherafati, R. Mirzazadeh, E. Barzegari, M. Mohammadi-Khanaposhtani, H. Azizian, M. S. Asgari, S. Hosseini, E. Zabihi, S. Mojtabavi and M. A. Faramarzi, *Bioorg. Chem.*, 2021, **109**, 104703.
28 M. Sohrabi, M. Saeedi, B. Larijani and M. Mahdavi, *Eur. J. Med. Chem.*, 2021, 113308.
29 S. Maikoo, D. Makayane, I. N. Booysen, P. Ngubane and A. Khathi, *Eur. J. Med. Chem.*, 2020, 113064.
30 D. C. Crans and K. Kostenkova, *Commun. Chem.*, 2020, **3**, 1–4.
31 C. Van Cleave and D. C. Crans, *Inorganics*, 2019, **7**, 111.
32 G. Parkin, *J. Chem. Educ.*, 2006, **83**, 791.
33 H. Sakurai, A. Katoh, T. Kiss, T. Jakusch and M. Hattori, *Metallomics*, 2010, **2**, 670–682.
34 K. Thompson, V. Yuen, J. McNeill and C. Orvig, *ACS Symp. Ser.*, 1998, **711**, 329–343.
35 E. L. Tolman, E. Barris, M. Burns, A. Pansini and R. Partridge, *Life Sci.*, 1979, **25**, 1159–1164.
36 B. Lyonnet, *Presse Med.*, 1899, **1**, 191–192.
37 C. E. Heyliger, A. G. Tahiliani and J. H. McNeill, *Science*, 1985, **227**, 1474–1477.
38 K. H. Thompson and C. Orvig, *Met. Ions Biol. Syst.*, 2004, **41**, 221–252.
39 K. H. Thompson, J. H. McNeill and C. Orvig, *Chem. Rev.*, 1999, **99**, 2561–2572.
40 S. Dai, K. Thompson and J. McNeill, *J. Pharmacol. Toxicol.*, 1994, **74**, 101–109.
41 K. H. Thompson, B. D. Liboiron, Y. Sun, K. D. Bellman, I. A. Setyawati, B. O. Patrick, V. Karunaratne, G. Rawji, J. Wheeler and K. Sutton, *J. Biol. Inorg Chem.*, 2003, **8**, 66–74.
42 S. Fujimoto, H. Yasui and Y. Yoshikawa, *J. Inorg. Biochem.*, 2013, **121**, 10–15.
43 K. J. Kilpin and P. J. Dyson, *Chem. Sci.*, 2013, **4**, 1410–1419.
44 Y. Yoshikawa, E. Ueda, K. Kawabe, H. Miyake, H. Sakurai and Y. Kojima, *Chem. Lett.*, 2000, **29**, 874–875.
45 A. Rubenstein, N. Levin and G. Elliott, *Nature*, 1962, **194**, 188–189.
46 Y. Yoshikawa, E. Ueda, K. Kawabe, H. Miyake, T. Takino, H. Sakurai and Y. Kojima, *J. Biol. Inorg Chem.*, 2002, **7**, 68–73.
47 Y. Yoshikawa, E. Ueda, Y. Kojima and H. Sakurai, *Life Sci.*, 2004, **75**, 741–751.
48 L. Coulston and P. Dandona, *Diabetes*, 1980, **29**, 665–667.
49 R. Narang, B. Narasimhan and S. Sharma, *Curr. Med. Chem.*, 2012, **19**, 569–612.
50 F. Guo, T. Xia, P. Xiao, Q. Wang, Z. Deng, W. Zhang and G. Diao, *Bioorg. Chem.*, 2021, **110**, 104764.
51 T.-H. Duong, A. P. Devi, N.-V. Huynh, J. Sichaem, H.-D. Tran, M. Alam, T.-P. Nguyen, H.-H. Nguyen, W. Chavasiri and T.-C. Nguyen, *Bioorg. Med. Chem. Lett.*, 2020, **30**, 127359.
52 P. Akhter, U. Ashiq, R. A. Jamal, Z. Shaikh, M. Mahroof-Tahir, M. Lateef and R. Badar, *Med. Chem.*, 2019, **15**, 923–936.
53 S. Khan, M. Tariq, M. Ashraf, S. Abdullah, M. Al-Rashida, M. Khalid, P. Taslimi, M. Fatima, R. Zafar and Z. Shafiq, *Bioorg. Chem.*, 2020, **102**, 104082.
54 J. E. Philip, M. Shahid, M. P. Kurup and M. P. Velayudhan, *J. Photochem. Photobiol., B*, 2017, **175**, 178–191.

55 K. K. Naik, S. Selvaraj and N. Naik, *Spectrochim. Acta, Part A*, 2014, **131**, 599–605.
56 S. Barrie, J. Wright, J. Pizzorno, E. Kutter and P. Barron, *Agents Actions*, 1987, **21**, 223–228.
57 P. J. Aggett, P. K. Fenwick and H. Kirk, *J. Nutr.*, 1989, **119**, 1432–1437.
58 I. Krieger, R. Cash and G. W. Evans, *J. Pediatr. Gastroenterol. Nutr.*, 1984, **3**, 62–68.
59 R. Grant, S. Coggan and G. Smythe, *Int. J. Tryptophan Res.*, 2009, **2**, S2469.
60 L. Tan, J.-T. Yu and L. Tan, *J. Neurol. Sci.*, 2012, **323**, 1–8.
61 Y. Yoshikawa, R. Hirata, H. Yasui and H. Sakurai, *Biochimie*, 2009, **91**, 1339–1341.
62 D. Avcı, S. Altürk, F. Sönmez, Ö. Tamer, A. Başoğlu, Y. Atalay and B. Z. Kurt, *J. Mol. Struct.*, 2020, **1205**, 127655.
63 D. Avcı, S. Altürk, F. Sönmez, Ö. Tamer, A. Başoğlu, Y. Atalay, B. Z. Kurt and N. Dege, *J. Mol. Struct.*, 2019, **1197**, 645–655.
64 D. Avcı, S. Altürk, F. Sönmez, Ö. Tamer, A. Başoğlu, Y. Atalay, B. Z. Kurt and N. Dege, *Mol. Diversity*, 2020, 1–19.
65 N. Dege, Ö. Özge, D. Avcı, A. Başoğlu, F. Sönmez, M. Yaman, Ö. Tamer, Y. Atalay and B. Z. Kurt, *Spectrochim. Acta, Part A*, 2021, **262**, 120072.
66 D. Avcı, S. Altürk, F. Sönmez, Ö. Tamer, A. Başoğlu, Y. Atalay, B. Z. Kurt and N. Dege, *Tetrahedron*, 2018, **74**, 7198–7208.
67 D. Avcı, S. Altürk, F. Sönmez, Ö. Tamer, A. Başoğlu, Y. Atalay, B. Z. Kurt and N. Dege, *J. Biol. Inorg Chem.*, 2019, **24**, 747–764.
68 D. Avcı, S. Altürk, F. Sönmez, Ö. Tamer, A. Başoğlu, Y. Atalay, B. Z. Kurt and N. Dege, *Appl. Organomet. Chem.*, 2020, **34**, e5412.
69 L. Li, Q. Guo, J. Dong, T. Xu and J. Li, *J. Photochem. Photobiol., B*, 2013, **125**, 56–62.
70 S. Arulmurugan, H. P. Kavitha and B. Venkatraman, *Rasayan J. Chem.*, 2010, **3**, 385–410.
71 E. A. Bajema, K. Roberts and T. Meade, *Met. Ions Life Sci.*, 2019, **19**, 267–301.
72 R. Miyazaki, H. Yasui and Y. Yoshikawa, *Open J. Inorg. Chem.*, 2016, **6**, 114–124.
73 D. Lucet, T. Le Gall and C. Mioskowski, *Angew. Chem., Int. Ed.*, 1998, **37**, 2580–2627.
74 I. P. Tripathi, A. Dwivedi and M. Mishra, *Asian J. Med. Health*, 2017, **2**, 1–14.
75 I. Tripathi and A. Dwivedi, *J. Adv. Med. Med. Res.*, 2016, 1–11.
76 I. P. Tripathi, M. M. Kumar, K. Arti, M. Chinmayi, T. Ruchita, S. L. Kant and P. K. Bihari, *Res. J. Chem. Sci.*, 2013, **2231**, 606X.
77 N. N. Greenwood and A. Earnshaw, *Chemistry of the Elements*, Elsevier, 2012.
78 H. Marschner and V. Römheld, *Plant Soil*, 1994, **165**, 261–274.
79 W. T. Cefalu and F. B. Hu, *Diabetes Care*, 2004, **27**, 2741–2751.
80 R. A. Anderson, *J. Am. Coll. Nutr.*, 1998, **17**, 548–555.
81 K. Schwarz and W. Mertz, *Arch. Biochem. Biophys.*, 1959, **85**, 292–295.
82 K. N. Jeejeebhoy, R. Chu, E. Marliss, G. R. Greenberg and A. Bruce-Robertson, *Am. J. Clin. Nutr.*, 1977, **30**, 531–538.
83 E. Król, Z. Krejpcio, M. Okulicz and H. Śmigielska, *Biol. Trace Elem. Res.*, 2020, **193**, 185–194.
84 D. Avcı, S. Altürk, F. Sönmez, Ö. Tamer, A. Başoğlu, Y. Atalay, B. Z. Kurt and N. Dege, *J. Mol. Struct.*, 2020, **1220**, 128761.
85 L. R. Hassan, H. Bahron, F. Abdullah and A. M. Tajuddin, *J. Biol. Inorg Chem.*, 2020, **25**, 239–252.
86 N. D. Chasteen, J. K. Grady and C. E. Holloway, *Inorg. Chem.*, 1986, **25**, 2754–2760.
87 K. H. Thompson and C. Orvig, *J. Chem. Soc., Dalton Trans.*, 2000, 2885–2892.
88 C. Amante, D. Sousa-Coelho, A. Luísa and M. Aureliano, *Metals*, 2021, **11**, 828.
89 S. Selvaraj and U. M. Krishnan, *J. Med. Chem.*, 2021, **64**, 12435–12452.
90 A. Ścibior and J. Kurus, *Curr. Med. Chem.*, 2019, **26**, 5456–5500.
91 K. Cusi, S. Cukier, R. DeFronzo, M. Torres, F. Puchulu and J. P. Redondo, *J. Clin. Endocrinol. Metab.*, 2001, **86**, 1410–1417.
92 A. B. Goldfine, M.-E. Patti, L. Zuberi, B. J. Goldstein, R. LeBlanc, E. J. Landaker, Z. Y. Jiang, G. R. Willsky and C. R. Kahn, *Metabolism*, 2000, **49**, 400–410.
93 U. Ashiq, R. Ara, M. Mahroof-Tahir, Z. T. Maqsood, K. M. Khan, S. N. Khan, H. Siddiqui and M. I. Choudhary, *Chem. Biodiversity*, 2008, **5**, 82–92.
94 R. Patel and Y. P. Singh, *J. Mol. Struct.*, 2018, **1153**, 162–169.
95 S. Bharathi, D. Mahendiran, R. Senthil Kumar and A. Kalilur Rahiman, *ChemistrySelect*, 2020, **5**, 6245–6254.
96 S. Misra, K. B. Pandeya, A. K. Tiwari, A. Z. Ali, T. Saradamani, S. B. Agawane and K. Madhusudana, *Int. J. Nutr. Metab.*, 2012, **4**, 11–18.
97 T. V. Basova, N. S. Mikhaleva, A. K. Hassan and V. G. Kiselev, *Sens. Actuators, B*, 2016, **227**, 634–642.
98 T. Basova, E. Kol'tsov, A. Ray, A. Hassan, A. Gürek and V. Ahsen, *Sens. Actuators, B*, 2006, **113**, 127–134.
99 R. J. G. Rubira, P. H. B. Aoki, C. J. L. Constantino and P. Alessio, *Appl. Surf. Sci.*, 2017, **416**, 482–491.
100 T. Keleş, Z. Biyiklioglu, E. Güzel, M. Nebioğlu and İ. Şişman, *Appl. Organomet. Chem.*, 2021, **35**, e6076.
101 B. Yıldız, E. Güzel, D. Akyüz, B. S. Arslan, A. Koca and M. K. Şener, *Sol. Energy*, 2019, **191**, 654–662.
102 A. B. Sorokin, *Chem. Rev.*, 2013, **113**, 8152–8191.
103 P.-C. Lo, M. S. Rodríguez-Morgade, R. K. Pandey, D. K. Ng, T. Torres and F. Dumoulin, *Chem. Soc. Rev.*, 2020, **49**, 1041–1056.
104 F. Özen, A. Günel and A. Baran, *Bioorg. Chem.*, 2018, **81**, 71–78.
105 B. Barut and Ü. Demirbaş, *J. Organomet. Chem.*, 2020, **923**, 121423.
106 E. Güzel, Ü. M. Koçyiğit, P. Taslimi, S. Erkan and O. S. Taskin, *J. Biochem. Mol. Toxicol.*, 2021, **35**, 1–9.

107 A. Günsel, F. Kalkan, G. Y. Atmaca, B. Barut, A. T. Bilgiçli, H. Pişkin, A. Özel, A. Erdoğmuş and M. N. Yarasir, *Appl. Organomet. Chem.*, 2021, **35**, e6202.
108 Ü. M. Koçyiğit, P. Taslimi, B. Tüzün, H. Yakan, H. Muğlu and E. Güzel, *J. Biomol. Struct. Dyn.*, 2020, 1–11.
109 A. Günsel, P. Taslimi, G. Y. Atmaca, A. T. Bilgiçli, H. Pişkin, Y. Ceylan, A. Erdoğmuş, M. N. Yarasir and İ. Gülçin, *J. Mol. Struct.*, 2021, **1237**, 130402.
110 A. Günsel, A. T. Bilgicli, B. Barut, P. Taslimi, A. Özel, İ. Gülçin, Z. Biyiklioglu and M. N. Yarasir, *J. Mol. Struct.*, 2020, **1214**, 128210.
111 F. Türkan, P. Taslimi, B. Cabir, M. S. Ağırtaş, Y. Erden, H. U. Celebioglu, B. Tuzun, E. Bursal and I. Gulcin, *Polycyclic Aromat. Compd.*, 2021, 1–13.
112 A. Günsel, A. Yıldırım, P. Taslimi, Y. Erden, T. Taskin-Tok, H. Pişkin, A. T. Bilgiçli, İ. Gülçin and M. N. Yarasir, *Inorg. Chem. Commun.*, 2022, **138**, 109263.
113 B. Barut, T. Keleş, Z. Biyiklioglu and C. Ö. Yalçın, *Appl. Organomet. Chem.*, 2021, **35**, e6021.
114 E. Güzel, Ü. M. Koçyiğit, B. S. Arslan, M. Ataş, P. Taslimi, F. Gökalp, M. Nebioğlu, İ. Şişman and İ. Gulçin, *Arch. Pharm.*, 2019, **352**, 1800292.
115 Y. Wang, L. Ma, Z. Li, Z. Du, Z. Liu, J. Qin, X. Wang, Z. Huang, L. Gu and A. S. Chen, *FEBS Lett.*, 2004, **576**, 46–50.